1 Influence of oceanic ventilation and terrestrial transport on the atmospheric

- 2 volatile chlorinated hydrocarbons over the Western Pacific
- 3 Shan-Shan Liu ^{1,2,#}, Jie Ni ^{1,#}, Jin-Ming Song ², Xu-Xu Gao ¹, Zhen He ^{1,3,*},
- 4 Gui-Peng Yang 1,3,4,*
- ⁵ Frontiers Science Center for Deep Ocean Multispheres and Earth System, and
- 6 Key Laboratory of Marine Chemistry Theory and Technology, Ministry of
- 7 Education, Ocean University of China, Qingdao 266100, China
- 8 ² Key Laboratory of Marine Ecology and Environmental Sciences, Institute of
- 9 Oceanology, Chinese Academy of Sciences, Qingdao 266071, China
- ³ Laboratory for Marine Ecology and Environmental Science, Qingdao Marine
- Science and Technology Center, Qingdao 266237, China
- ⁴ Institute of Marine Chemistry, Ocean University of China, Qingdao 266100,
- 13 China
- [#]Shan-Shan Liu and Jie Ni contributed equally to the paper.
- *Corresponding author: zhenhe@ouc.edu.cn (Z. He), gpyang@mail.ouc.edu.cn
- 16 (G.-P. Yang)

17 Abstract

- Volatile chlorinated hydrocarbons (VCHCs), key ozone-depleting substances
- 19 and greenhouse gases, depend on oceanic emission and uptake for their
- 20 atmospheric budget. However, data on VCHCs in the Western Pacific remain
- 21 limited. This study investigated the distribution and sources of VCHCs (CHCl₃,
- 22 C₂HCl₃, CCl₄, and CH₃CCl₃) in the Western Pacific during 2019-2020. Elevated
- 23 seawater concentrations of CHCl₃ and C₂HCl₃ in the Kuroshio-Oyashio Extension
- 24 were driven by mesoscale eddies, enhancing primary productivity, while CCl₄ and
- 25 CH₃CCl₃ concentrations were mainly influenced by atmospheric inputs.

Atmospheric concentrations of VCHCs decreased from coastal to open ocean areas, with terrestrial air masses contributing significantly. Additionally, positive saturation anomalies and correlations with chlorophyll-a indicated the marine biological source for atmospheric CHCl₃ and C₂HCl₃. However, the atmospheric concentration variability of these gases was not fully consistent with oceanic emissions indicators (saturation anomalies and sea-air fluxes) and showed strong correlations with terrestrial tracers, indicating that land-derived atmospheric transport primarily influenced atmospheric CHCl₃ and C₂HCl₃. The estimated sea-air flux indicated that the Western Pacific acted as a source for CHCl3 and C_2HCl_3 but a sink for CCl_4 and CH_3CCl_3 , with the potential to absorb $14.3 \pm 6.8\%$ of CCl₄ emissions from Eastern China, $5.6 \pm 2.5\%$ from Eastern Asia, and $2.1 \pm$ 1.1% of global emissions. Additionally, this region accounted for $6.3 \pm 2.8\%$ of the global oceanic absorption of CCl₄. These findings underscore the Western Pacific's key role in regulating atmospheric CCl₄ concentrations and mitigating its accumulation in Eastern Asia, providing essential data for global VCHCs emission and uptake estimates.

26

27

28

29

30

31

32

33

34

35

36

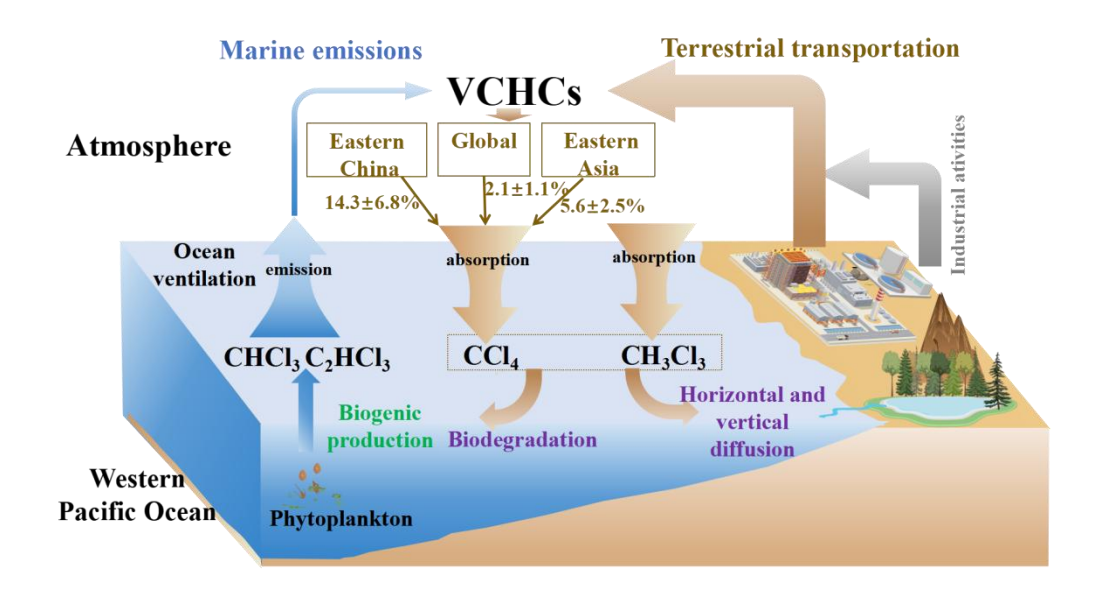
37

38

39

40

42 Graphical abstract



Introduction

43

44

45

46

47

48

49

50

51

52

53

54

55

56

57

58

59

Volatile halocarbons (VHCs) are ozone-depleting substances greenhouse gases (Abrahamsson et al., 1995; Abrahamsson and Edkahl, 1996). As an important component of VHCs, volatile chlorinated hydrocarbons (VCHCs) are believed to be important carriers of chlorine to the stratosphere. Among them, carbon tetrachloride (CCl₄), chloroform (CHCl₃), methyl chloroform (CH₃CCl₃), and trichloroethene (C₂HCl₃) account for an estimated 11% of the total organic chlorine in the troposphere (WMO, 2022). Long-lived compounds such as CCl₄ and CH₃CCl₃, which have atmospheric lifetimes exceeding six months, are well-mixed in the troposphere except where there are local sources. They are major contributors to both the greenhouse effect and ozone depletion, and their usage and emissions are subject to regulation under the Montreal Protocol (1987). In contrast, short-lived species such as C₂HCl₃ and CHCl₃ are classified as halogenated very short-lived substances (VSLSs), with typical atmospheric lifetimes of less than six months (WMO, 2007), and are currently not regulated under the Montreal Protocol. Nevertheless, a significant portion of VSLSs and 60 their degradation products reach the stratosphere, with over 80% of chlorinated VSLSs estimated to reach these altitudes (Carpenter et al., 2014). Although present 61 62 at low concentrations, VSLSs exert disproportionately large impacts on radiative forcing and climate through ozone depletion, particularly due to their breakdown 63 in the lower atmosphere, which is more sensitive to climate change (Hossaini et al., 64 2015, 2017; An et al., 2023; Saiz-Lopez et al., 2023). 65 66 The oceans, acting as source and sink of VCHCs (C₂HCl₃, CHCl₃, CCl₄, and CH₃CCl₃), play a significant role in the biogeochemical cycling of VCHCs (Blake 67 68 et al., 2003; Karlsson et al., 2008; Butler et al., 2016). CHCl₃ and C₂HCl₃ in the oceans come from both anthropogenic and natural sources (Abrahamsson and 69 Edkahl, 1996; Moore, 2003; Karlsson et al., 2008; He et al., 2013c). Previous 70 71 studies have revealed that marine microalgae (Scarratt et al., 1999; Lim et al., 2018), macroalgae (Gschwend et al., 1985; Abrahamsson et al., 1995), and various 72 other marine organisms (Khan et al., 2011) act as natural sources of CHCl₃ and 73 C₂HCl₃. The tropical diatoms, the cyanobacterium Synechococcus and the 74 chlorophyte Parachlorella, and purple sulfur bacteria, have been shown to produce 75 CHCl₃ (Scarratt et al., 1999; Plummer et al., 2002; Lim et al., 2018). Moreover, 76 CHCl₃ emissions have also been found in regions like the Antarctic tundra (Zhang 77 et al., 2021), Dead Sea landscapes (Shechner et al., 2019), and coastal wetlands 78 79 affected by sea level rise (Jiao et al., 2018), entering the ocean via land runoff and atmospheric deposition. Abrahamsson et al. (1995) argued that C₂HCl₃ emissions 80 from algae to the atmosphere are present in non-negligible amounts within the 81 82 global atmospheric chlorine budget. Anthropogenic emissions of CHCl₃ mainly

come from its use as a raw material in refrigerant hydrochlorofluorocarbon-22

(HCFC-22) production and as a byproduct of the water chlorination and bleaching

83

processes in the pulp and paper industry (McCulloch, 2003). C₂HCl₃ is also emitted from its use as a solvent and as feedstock in producing HFCs and other chemicals (Chipperfield et al., 2020). Notably, while the Montreal Protocol regulates the use of HCFC-22 in dispersive applications, demand for the refrigerant as a feedstock in the manufacture of fluoropolymers is surging (Say et al., 2020). These anthropogenic CHCl₃ and C₂HCl₃ ultimately enter the ocean through land runoff and atmospheric deposition, especially in coastal and estuarine regions (Yokouchi et al., 2005). In contrast, oceanic CH₃CCl₃ and CCl₄ are largely from anthropogenic sources (Butler et al., 2016; WMO, 2022). As a primary component of cleaning agents, dry-cleaning solvents, and degreasing agents, CH₃CCl₃ previously saw widespread use (Wang et al., 1995). CCl₄ was previously extensively used in chlorine gas production, industrial bleaching, organic chemical solvents, and fire extinguisher production (Rigby et al., 2014). Moreover, these two gases are used as solvents and feedstock chemicals in producing HFCs and other chemicals (Chipperfield et al., 2020). Although their usage is banned in the Montreal Protocol (1987) and its amendments and adjustments, unregulated emissions persist from specific manufacturing activities. For example, Liang et al. (2016) and Sherry et al. (2018) showed that CCl₄ production is linked to non-feedstock emissions associated with chloromethane and perchloroethylene manufacturing facilities. They also demonstrated that up to 10 Gg yr⁻¹ of CCl₄ emissions may be produced by unreported, unintentional release during chlorine production, including emissions from chlor-alkali plants and their use in industrial and domestic bleaching. Additionally, Li et al. (2024) identified potential CCl₄ sources in eastern China, including the manufacture of general-purpose machinery, raw chemical materials, and chemical products.

85

86

87

88

89

90

91

92

93

94

95

96

97

98

99

100

101

102

103

104

105

106

107

108

Substantial spatial and temporal variabilities characterize the distributions of VCHCs in oceans, with higher concentrations in estuaries than nearshore zones, and higher concentrations in nearshore zones than in the open ocean. These distributions are mainly influenced by anthropogenic emissions from terrestrial sources (Yokouchi et al., 2005; Bravo-Linares et al., 2007; Liang et al., 2014) and by the biological processes of algae in nearshore zones (Christof et al., 2002; Karlsson et al., 2008; Yang et al., 2015). In addition, the distributions of VCHCs are related to various factors, including source strength, season, topography, tides, and water masses (Yang et al., 2015; Liu et al., 2021). Previous studies have pointed out that land-based inputs have significant impacts on the distributions of marine VCHCs because VCHCs from human activities exceed marine emissions (Lunt et al., 2018; Fang et al., 2019; An et al., 2021; Yi et al., 2023). For example, persistent large emissions of CCl₄ from Eastern Asia, accounting for approximately 40% of global emissions (Lunt et al., 2018), coincided with a global increase in CCl₄ mole fractions between 2010 and 2015, as noted by Fang et al. (2019). This growth, notably driven by eastern China, has potential implications for Antarctic ozone layer recovery. However, according to the latest data from WMO (2022), the CCl₄ emissions from eastern China showed a significant decline from 2016 to 2019, dropping from 11.3 ± 1.9 Gg yr⁻¹ in 2016 to 6.3 ± 1.1 Gg yr⁻¹ in 2019. Similarly, An et al. (2023) reported a decline in CHCl₃ emissions from China, which peaked at 193 Gg yr⁻¹ in 2017 and decreased to 147 Gg yr⁻¹ by 2018, where, as of 2020, it has remained relatively constant. Yu et al. (2020) demonstrated a successful reduction in China CH₃CCl₃ emissions from 1.6 Gg yr⁻¹ in 2007 to 0.3 Gg yr⁻¹ in 2013, demonstrating compliance with the Montreal Protocol. Despite these declines in VCHCs emissions, Eastern Asia continues to be

110

111

112

113

114

115

116

117

118

119

120

121

122

123

124

125

126

127

128

129

130

131

132

133

an important source of global VCHCs emissions (WMO, 2022).

The Western Pacific exerts a profound influence on sea-air exchanges and the

135

136

137

138

139

140

141

142

143

144

145

146

147

148

149

150

151

152

153

154

155

156

157

158

159

global biogeochemical cycles of materials (Tsunogai, 2002; Shi et al., 2022). The dynamic western boundary currents, equatorial Pacific circulation systems, and the expansive Western Pacific Warm Pool play pivotal roles in vertical water mass transport and material/heat exchange between the equatorial and subtropical Pacific regions (Hu et al., 2015). These oceanic processes likely impact the variations in emissions of VCHCs in the Western Pacific. Additionally, owing to its proximity to land, encompassing regions such as the Philippines and Japan, atmospheric vertical diffusion and pollutant transport from land may significantly influence atmospheric VCHCs levels over the Western Pacific (Lunt et al., 2018). While a few studies have observed seawater and atmospheric VCHCs in the Western Pacific (Quack and Suess, 1999; Liu et al., 2021), comprehensive data on atmospheric and seawater VCHCs in the Western Pacific remain scarce. Consequently, substantial uncertainties persist in estimates of oceanic sources and sinks of VCHCs (Blake et al., 2003; Butler et al., 2016). A noticeable research gap exists concerning our understanding of VCHCs in the Western Pacific. Furthermore, the lack of comprehensive knowledge regarding the biogeochemical factors that control VCHCs concentrations and sea-air fluxes produces uncertainties in global emission estimates. In this study, a comprehensive field investigation was carried out in the Western Pacific with two primary objectives. Firstly, the study aimed to understand how oceanic physical and biogeochemical processes influence the distributions and emissions of these climatic VCHCs by examining various sources. Secondly, the study sought to ascertain the influence of the Western Pacific on the levels of volatile VCHCs in the atmosphere, evaluating whether it acts primarily as a source or sink of these VCHCs. Investigating the distributions of VCHCs in both the seawater and the atmosphere, along with determining their sea—air fluxes, is essential for evaluating their potential impacts on the global halogen cycle.

2 Materials and methods

2.1 Study area

160

161

162

163

164

165

166

167

168

169

170

171

172

173

174

175

176

177

178

179

180

181

182

183

184

Our measurements were conducted on board the R/V "Dongfanghong 3" from October 31 to December 1, 2019, and the R/V "Science" from October 3, 2019, to January 5, 2020. A total of 65 stations were surveyed across the study region (Fig. 1a), where seawater samples were collected at all stations and atmospheric samples obtained at 41 stations. Each station provided three replicate surface seawater samples and one atmospheric sample. The Western Pacific survey area was divided into the Kuroshio-Oyashio Extension (KOE), North Pacific Subtropical Gyre (NPSG), and Western Pacific Warm Pool (WPWP) based on oceanographic features, including seawater temperature, salinity, nutrient concentrations, and Chl-a concentrations observed in this study (Fig. S1 and Fig. S2). Details of the classification criteria are given in the Supplementary Information (Text S1). The cruises encompassed a broad geographic range, extending from coastal to open-ocean areas and from tropical to subtropical latitudes. Data were collected along multiple transects, summarized here along two primary directions: the South-North (S-N) direction (from 1°S to 40°N) and the East-West (E-W) direction (from 130°E to 165°E). The circulation patterns of the Western Pacific, depicted in Fig. 1b, are intricate and encompass multiple oceanic currents, including the Oyashio Current (OC), the North Equatorial Current (NEC), the North Equatorial Counter Current (NECC), the Mindanao Current (MC), and the Kuroshio Current (KC). This intricate marine circulation system and the intense ocean-atmosphere interactions bestow the Western Pacific with a pivotal role in oceanic environmental changes, water mass exchanges, nutrient and heat transport, global biogeochemical cycles, and climatic transitions (Hu et al., 2020). Further, with the planet's largest warm pool and most robust tropical convection, the WPWP area is a critical player in global sea—air substance exchange. Meteorological patterns in this area are also significantly influenced by the Indo-Australian monsoon (Wang et al., 2004; Li et al., 2019). Thus, the combined forces of the NEC-MC-KC system and the region's distinct meteorological conditions inevitably modulate the biogeochemical cycling of VCHCs in both seawater and the atmosphere.

2.2 Analysis of VCHCs in air

Atmospheric samples were collected by 3 L pre-evacuated stainless-steel Summa polished canisters (SilconCan, Restek Co., Ltd) that were pre-cleaned to measure VCHCs concentrations at ambient pressure. These sampling canisters underwent an intensive cleaning process using an automated cleaning system (Nutech 2010 DS) prior to sample collection. Previous studies have shown that VCHCs remain stable in rigorously pre-cleaned Summa canisters for more than 3 months (Yokouchi et al., 1999; Yokouchi et al., 2013; Yu et al., 2020). To avoid ship exhaust contamination, sampling was conducted upwind on the ship's top deck during low-speed transit. All atmospheric samples were analyzed within 3 months after the collection. Meteorological parameters such as wind speed and direction were recorded by shipboard sensors at a height of 10 m above the sea surface.

The atmospheric concentrations of VCHCs were determined using a three-stage cold-trap preconcentrator (Nutech 8900DS) coupled with a gas chromatography-mass spectrometry (GC-MS) system (Agilent 7890A/5975C). Chromatographic separation was achieved on a DB-624 capillary column (60 m × $0.25 \text{ mm} \times 1.4 \mu\text{m}$ film thickness) in selective ion monitoring (SIM) mode. Prior to injection, samples (400 mL) were preconcentrated using the three-stage cold-trap system, effectively removing interfering components such as H₂O and CO₂. Target compounds were quantified using a multipoint external calibration method. Calibration curves were established with a 100 ppbv mixed standard gas (Spectra Gases, USA), which was dynamically diluted with ultra-high-purity nitrogen using a mass-flow-controlled dilution system (Nutech 2202A; accuracy $\pm 1\%$) to achieve pptv-low ppbv concentration levels. Six concentration gradients were prepared, and the diluted standards were analyzed following the same procedures as the field samples. The calibration results showed correlation coefficients for all target compounds are ≥ 0.996 . According to the US EPA (2019) procedure, the method detection limits (MDL) of the target compounds ranged from 0.10 to 1.0 pptv. MDL is defined as 3.143 × standard deviation of seven replicates of the low concentration standard gases (5 × the expected MDL), where 3.143 represents the t-value at 99% confidence level. Precision in this study was assessed from seven replicate measurements of standard gas samples prepared at environmentally relevant concentrations, with relative standard deviations (RSD) consistently below 7% for all target compounds (Table S1). This method has been validated through comparisons with the China Meteorological Administration Meteorological Observation Centre for independent analysis using an AGAGE-traceable Medusa-GC/MS system (Zhang et al., 2017; Yu et al., 2020; An

210

211

212

213

214

215

216

217

218

219

220

221

222

223

224

225

226

227

228

229

230

231

232

233

et al., 2021). Furthermore, it is consistent with previously published methodologies (Zhang et al., 2010; Zheng et al., 2013; Yi et al., 2021; Li et al., 2024). Detailed analytical procedures and data processing methods are provided in the Supplementary Information (Text S2 and Text S3).

2.3 Analysis of VCHCs in seawater

235

236

237

238

239

240

241

242

243

244

245

246

247

248

249

250

251

252

253

254

255

256

257

258

259

Surface seawater (5 m) was collected using a 12 L Niskin sampler equipped with a temperature-salinity-depth probe (CTD) for concurrent temperature and salinity measurements. Samples were transferred into 100 mL airtight glass syringes without headspace, stored in the dark at 4 °C, and analyzed within 4 h of collection. To minimize compound concentration changes, Samples for VCHCs were analyzed immediately onboard using a cold trap purge-and-trap gas chromatograph equipped with an electron capture detector (GC-ECD, Agilent 6890A). Briefly, seawater samples (100 mL) were transferred to a purge-and-trap apparatus and purged with high-purity nitrogen at a flow rate of 60 mL min⁻¹ for 14 min. The purged VCHCs were sequentially passed through glass tubes containing magnesium perchlorate (MgClO₄) and sodium hydroxide (NaOH) for drying and CO₂ removal, followed by enrichment onto a trap column (length: 30 cm; diameter: 0.8 mm) immersed in liquid nitrogen. After trapping, the trap was subsequently heated with boiling water, and the desorbed gases were introduced into the GC using high-purity nitrogen. Separation was performed on a DB-624 capillary column (60 m \times 0.53 mm \times 3.0 μ m film thickness) with the following temperature program: 45 °C (hold 10 min), ramp to 200 °C at 15 °C min⁻¹, and hold for 5 min. The inlet and detector temperatures were 110 °C and 275 °C, respectively, and the carrier gas (ultrapure N₂) flow rate was 2.1 mL min⁻¹.

Identification and quantification of the VCHCs in seawater were based on

retention times and liquid standards purchased from o2si in the US (purity > 99%). The liquid standards were diluted twice with methanol (Merck, Darmstadt, Germany, suitable for purging and analysis) to obtain the desired standard concentrations. Using the same analytical method as for the surface seawater samples, the deep seawater (5000 m) was purged with high-purity N_2 to remove the background VCHCs, and standard curves were established by diluting VCHCs standards in series (correlation coefficients > 0.995). The detection limits for target compounds in this method ranged between 0.05 pmol L^{-1} and 0.50 pmol L^{-1} with a relative standard deviation of 3% to 9% (He et al., 2013b, 2013c).

2.4 Determination of chlorophyll a (Chl-a) in seawater

For the analysis of Chl-*a*, seawater samples (500 mL) were vacuum-filtered through a 0.7 μm Whatman GF/F glass fiber filter (diameter: 47 mm) and stored in the dark at -20 °C. Upon transport to the laboratory, the samples were extracted in the dark with 10 mL of 90% acetone for 24 h and centrifuged at 4000 rpm for 10 min. The supernatant was then analyzed using a fluorescence spectrophotometer (F-4500, Hitachi), achieving a detection limit of 0.01 μg L⁻¹.

2.5 Calculation of sea-air fluxes and saturation anomalies

The sea-air fluxes of VCHCs, denoted by F (nmol m⁻² d⁻¹), were calculated according to the following equation.

$$F = k_w \left(C_w - C_a / H \right) \tag{1}$$

Where k_w (m d⁻¹) is the gas exchange constant. C_w and C_a are the concentrations of VCHCs in surface seawater and the atmosphere, respectively. H is the dimensionless Henry's Law constant, calculated as the equation of seawater temperature (T, in Kelvin). Specifically, the H values for CHCl₃ and C₂HCl₃ were derived from seawater-based temperature–H parameterizations reported by Moore

285 (2000). The H value for CCl₄ was obtained from the seawater-based equation of 286 Hunter-Smith et al. (1983). For CH₃CCl₃, the temperature dependence was taken 287 from the freshwater measurements of Schwardt et al. (2021) and subsequently 288 adjusted to seawater conditions using the Sechenov "salting-out" relationship, with 289 the salting-out coefficient (k_s) reported by Gossett (1987). The corresponding 290 equations are:

291
$$H(CHCl_3) = \exp(13.10 - 4377 \text{ T}^{-1})$$
 (2)

292
$$H(C_2HCl_3) = \exp(14.88 - 4624 \text{ T}^{-1})$$
 (3)

293
$$H(CCl_4) = \exp(11.27 - 3230 \text{ T}^{-1})$$
 (4)

294
$$H(CH_3CCl_3) = \exp(459.80 - 23465 T^{-1} - 66.96 Ln(T)) 1.305$$
 (5)

 k_w is calculated using the following equation by Wanninkhof (2014):

$$296 k_w = 0.251 \ u^2 \left(Sc \ / \ 660 \right)^{-1/2} (6)$$

Where u is the wind speed and Sc is the Schmidt constant. The Sc values of

VCHCs were calculated using the equation proposed by Khalil et al. (1999):

298

300

301

302

303

304

306

307

308

309

$$S_c = 335.6 M^{1/2} \times (1 - 0.065 t + 0.002043 t^2 - 2.6 \times 10^{-5} t^3)$$
 (7)

where t (°C) represents the temperature of the surface seawater and M is the molecular weight of VCHCs.

Saturation anomalies Δ (%) were calculated as the departure of the observed dissolved amount from equilibrium with air according to the following equation (Kurihara et al., 2010).

305
$$\Delta\% = 100 (C_w - C_a/H) / C_a/H$$
 (8)

A positive saturation anomaly implies a net flux from the ocean to the air.

The uncertainty of the sea-air fluxes obtained in this study arises from both systematic and random measurement errors. Propagation of error analysis was conducted to quantify the uncertainty of the calculated sea-air fluxes, following

the method outlined by Shoemaker et al. (1974).

311
$$\sigma^{2}F = \left(\frac{\partial F}{\partial k_{w}}\right)^{2} \left(\sigma k_{w}\right)^{2} + \left(\frac{\partial F}{\partial C_{w}}\right)^{2} \left(\sigma C_{w}\right)^{2} + \left(\frac{\partial F}{\partial C_{a}}\right)^{2} \left(\sigma C_{a}\right)^{2} + \left(\frac{\partial F}{\partial H}\right)^{2} \left(\sigma H\right)^{2}$$
(9)

The precision of VCHCs measurements was under 9%, determined based on repeated sample injections. The overall error was calculated at approximately 20%, primarily due to the value of 20% from Wanninkhof (2014) for uncertainty in k_w , influenced by wind speed and Sc variabilities. Also, while a single Henry's Law calculation was done, there is uncertainty in both the determination of H and the temperature dependence. Thus, the error of the flux estimate in this study was determined to be > 20%.

2.6 Data analysis

The Hybrid Single Particle Lagrangian Integrated Trajectory (HYSPLIT) model, provided by the National Oceanic and Atmospheric Administration (NOAA) (http://www.arl.noaa.gov/ready.php), was employed to generate 96 h backward trajectories for air masses. The Matlab software was used to compile and analyze all survey station back trajectories. The TrajStat module for the MeteoInfo software was applied for trajectory analysis, enabling the clustering of trajectories based on geographic origins and historical paths identified in a previous study (Squizzato and Masiol, 2015). Following convention (Byčenkienė et al., 2014; Liu et al., 2017), these trajectories were initialized 100 m above sea level. Meteorological data were obtained from the Global Data Assimilation System (GDAS) dataset (http://ready.arl.noaa.gov/archives.php).

3 Results and discussion

3.1 Variability of the overlying atmospheric VCHCs concentrations

The atmospheric mixing ratios of the four VCHCs over the Western Pacific

are summarized in Fig. 2, Fig. 3, and Fig. S3. The results indicated that the distributions of the selected VCHCs were correlated with both source strength and prevailing meteorological conditions. To clarify the drivers behind the observed concentration fluctuations and spatial patterns, the trace gases were classified into two groups based on their molecular lifetimes (Table S1).

3.1.1 CCl₄ and CH₃CCl₃

334

335

336

337

338

339

340

341

342

343

344

345

346

347

348

349

350

351

352

353

354

355

356

357

358

Atmospheric concentrations of CCl₄ and CH₃CCl₃ over the Western Pacific varied from 75.8 to 83.7 pptv (mean: 78.8 pptv) and from 1.6 to 2.4 pptv (mean: 2.0 pptv), respectively (Fig. 3 and Fig. S3). The concentration of CCl₄ was similar to the average background mixing ratio of 78.5 pptv in the Northern Hemisphere during a survey from October 2019 to January 2020, as reported by the AGAGE network (https://agage.mit.edu/). However, it was considerably lower than the concentrations reported by Blake et al. (2003) for the Pacific Ocean (108.7 pptv) from February 24 to April 10, 2001, the measurements by Zhang et al. (2010) in 2007 for the Pearl River Delta region (116 pptv), those by Ou-Yang et al. (2017) in 2015 for the Mt. Fuji Research Station in Japan (84 pptv), and by Zheng et al. (2019) in 2015 at the Yellow River delta in China (109 pptv). Similarly, the mean CH₃CCl₃ concentration in this study (2.0 pptv) exceeded the average background mixing ratio of 1.67 pptv in the Northern Hemisphere during a survey from October 2019 to January 2020 (https://agage.mit.edu/). However, the level reported here was lower than the concentration reported by He et al. (2013c) for the East China Sea (9.1 pptv) from May 2 to 9, 2012. Similarly, it was considerably lower than those reported by Blake et al. (2003) for the Pacific Ocean (132 pptv) from February 24 to April 10, 2001. It was also lower than the observed concentrations in the Pearl River Delta region (53 pptv) from October 25 to

December 1, 2007, by Zhang et al. (2010); the Mt. Fuji Research Station in Japan (4.0 pptv) from August 12 to August 17, 2015, by Ou-Yang et al. (2017); and the Yellow River Delta region, Northern China (2.8 pptv) from June 8 to July 9, 2017, by Zheng et al. (2019). These discrepancies likely reflect temporal variability in emissions and changes in the global burden, as well as differences in the sampling locations. Most samples in this study were collected in regions less influenced by continental outflow, resulting in relatively low concentrations.

Figure 3 shows the spatial distributions of atmospheric mixing ratios of CCl₄ and CH₃CCl₃. Significant enhancements were observed at nearshore stations (e.g., P1-4, P1-5, P1-7, P1-8 and EQ12). CCl₄ concentrations in these stations were 4–6% higher than the regional average, exceeding its analytical precision threshold of 3σ (3.3%, Table S1). These enhancements exhibited clear spatial consistency, systematically concentrated in nearshore areas influenced by continental air masses (Fig. 1c and Fig. 3). Moreover, the elevated levels coincided with enhanced concentrations of the independent anthropogenic tracer SF₆ (Ni et al., 2023), further corroborating their origin from continental pollution outflows. This result is also consistent with previous studies reporting that elevated CCl₄ and CH₃CCl₃ levels are primarily concentrated in coastal regions (Blake et al., 2003; Zhang et al., 2010).

In this study, the highest atmospheric concentrations of CCl₄ and CH₃CCl₃ were recorded at station P1-4 near Japan. Backward trajectory cluster analysis (Fig. 1c and Fig. S4) indicated that approximately 13% of the air masses originated from short-range transport along the eastern coast of Japan, while the remaining 87% were associated with long-range transport from Siberia and Northeast China and subsequently passed over the eastern coast of Japan. Although Siberia and

Northeast China are not typical source regions for halocarbons, previous studies have shown that air masses from these regions may mix with pollution plumes from East Asian industrial areas during long-range transport (Stohl et al., 2002; Blake et al., 2003; Liang et al., 2004; Chang et al., 2022), which could lead to elevated VCHCs concentrations at downwind observation stations. This is corroborated by reports of CCl₄ pollution events at the Shangdianzi (SDZ) regional background station in Northern China (117.17°E, 40.65°N, Fig. 1a), with peak mixing ratios reaching 151 pptv (Yi et al., 2023). As anthropogenic compounds, CCl₄ and CH₃CCl₃ are primarily emitted from industrial activities, including chloromethane and perchloroethylene production (Liang et al., 2016; Sherry et al., 2018), as well as unreported releases from chlorine and bleaching processes (estimated up to 10 Gg yr⁻¹). Furthermore, Zheng et al. (2019) and Ou-Yang et al. (2017) reported elevated CCl₄ and CH₃CCl₃ levels in China and Japan, respectively. Lunt et al. (2018) identified continued CCl₄ emissions from Eastern Asia. Collectively, these findings suggested that continental air mass transport was likely the dominant factor driving the elevated CCl₄ and CH₃CCl₃ levels observed at station P1-4 during the study period. In contrast, the lowest CCl₄ and CH₃CCl₃ concentrations were observed at station P1-24, where all affecting air mass trajectories came from the Pacific Ocean (Fig. 1c and Fig. S4), indicating the influence of clean marine background air (Fig. 1c).

3.1.2 CHCl₃ and C₂HCl₃

384

385

386

387

388

389

390

391

392

393

394

395

396

397

398

399

400

401

402

403

404

405

406

407

408

The atmospheric mixing ratios of CHCl₃ and C₂HCl₃ over the Western Pacific ranged from 6.0 to 29.4 pptv (mean: 12.4 ± 5.7 pptv) and from 1.1 to 3.4 pptv (mean: 2.0 ± 0.7 pptv), respectively. The concentration of CHCl₃ measured in the current work was similar to the average background mixing ratio of 11.82 pptv

409 measured in the Northern Hemisphere during the survey period from October 2019 to January 2020, as reported by AGAGE network (https://agage.mit.edu/). 410 411 However, it was lower than values reported from other areas, such as in a Western Pacific marginal sea—the South Yellow Sea—from May 2 to 9, 2012 (27.3 pptv; 412 He et al., 2013c), the Mt. Fuji Research station of Japan from August 12 to August 413 17, 2015 (39 \pm 11 pptv; Ou-Yang et al., 2017), and the Yellow River Delta region, 414 415 Northern China, from June 8 to July 9, 2017 (283 pptv; Zheng et al., 2019). The measurements of C2HCl3 were lower than in areas close to land sources, such as 416 417 the South Yellow Sea from May 2 to 9, 2012 (27.3 pptv; He et al., 2013c) and the Yellow River Delta region, Northern China, from June 8 to July 9, 2017 (20 pptv; 418 419 Zheng et al., 2019). This difference could be attributed to the surveyed area being 420 a relatively open sea, where the dilution effect by air from the marine boundary 421 layer (MBL) is more pronounced. Furthermore, the air in the study area is more photochemically aged, leading to lower observed values of C₂HCl₃. 422 Spatially, elevated concentrations of atmospheric CHCl₃ and C₂HCl₃ were 423 detected in nearshore regions, such as the KEO area and stations EQ12, E130-15, 424 and E130-18 (Fig. 2 and Fig. 3). Both CHCl₃ and C₂HCl₃ showed significant 425 correlations with SF₆ (r = 0.56, n = 38, p < 0.01 and r = 0.54, n = 38, p < 0.01, 426 respectively; Fig. S5). The result indicated that the high concentrations of these 427 428 two gases in the atmosphere mainly originated from anthropogenic input, as SF₆ is an important indicator of terrigenous sources. The 96-h backward trajectory cluster 429 analysis revealed that the KEO region is affected by air masses originating from 430 Siberia, Northeast China, Korea, and Japan (Fig. 1c). While Siberia and Northeast 431 China themselves are not recognized as major VCHCs source regions, the 432 long-range air masses from these areas may have entrained polluted plumes during 433

their transport (Section 3.1.1). Indeed, surrounding regions are known to be significant emitters: Feng et al. (2019) reported a marked rise in China's CHCl₃ emissions in recent years, and An et al. (2023) further showed that emissions peaked at 193 Gg yr⁻¹ in 2017 before declining to 147 Gg yr⁻¹ in 2018 and remaining stable thereafter, with eastern China consistently identified as a major contributor. Moreover, Ou-Yang et al. (2017) observed high atmospheric CHCl₃ mixing ratios (39 \pm 11 pptv) at the Mt. Fuji research station, Japan, in 2015; and in 2017, the highest annual mean CHCl₃ (43 \pm 18 pptv) was recorded at the Gosan station (GSN, 127.17°E, 33.28°N, 72 m above sea level, a regional baseline station; Fig. 1a) on Jeju Island, South Korea. Furthermore, industrial activities are known sources of CHCl₃ and C₂HCl₃ (Montzka et al., 2011; Oram et al., 2017; Zheng et al., 2019). Thus, the elevated CHCl₃ and C₂HCl₃ observed in the KEO region were likely related to terrestrial air mass transport and subsequent mixing with polluted plumes during their transit. In addition to terrestrial contributions, positive saturation anomalies of CHCl₃ and C₂HCl₃ in surface seawater (Fig. 4) indicated supersaturation, suggesting the oceanic emissions as a potential source of atmospheric CHCl₃ and C₂HCl₃. Previous studies have reported that substantial amounts of CHCl₃ and C₂HCl₃ are released from marine macroalgae and microalgae (Abrahamsson et al., 1995; Abrahamsson et al., 2004a; Chuck et al., 2005; Ekdahl et al., 1998; Lim et al., 2018) and subsequently transferred to the atmosphere via sea-air diffusion. Consistent with this, atmospheric CHCl₃ and C₂HCl₃ exhibited significant positive correlations with Chl-a levels in the study area (r = 0.83 and 0.58, p < 0.01, n=41; Fig. S6), supporting a potential biological contribution. Nevertheless, atmospheric levels of CHCl₃ and C₂HCl₃ were not fully consistent with oceanic emissions

434

435

436

437

438

439

440

441

442

443

444

445

446

447

448

449

450

451

452

453

454

455

456

457

indicators (saturation anomalies and sea–air fluxes). In the KOE region, where atmospheric mixing ratios and Chl-*a* were elevated, their saturation anomalies were relatively low compared to other regions (Fig. 4), and estimated sea–air fluxes showed no significant enhancement (Fig. 5). Moreover, strong correlations between atmospheric concentrations of CHCl₃ and C₂HCl₃ with terrestrial tracers (CCl₄, CH₃CCl₃, and SF₆; Fig. S6 and Fig. S7) suggested shared terrestrial sources or common atmospheric processes. Collectively, these results indicate that although marine biological production contributes to CHCl₃ and C₂HCl₃ emissions, terrestrial transport was the dominant factor controlling their atmospheric variability in the study region.

3.2 Regional characteristics of seawater VCHCs and their driving factors

The seawater distributions of CHCl₃, C₂HCl₃, CCl₄, and CH₃CCl₃ are shown in Fig. 2. Seawater CHCl₃, C₂HCl₃, CCl₄, and CH₃CCl₃ exhibited significant regional variability in the Western Pacific. Surface seawater concentrations of CHCl₃, C₂HCl₃, CCl₄, and CH₃CCl₃ in the KOE region were higher than those in the NPSG and WPWP (Fig. 2).

3.2.1 Kuroshio-Oyashio Extension

The KOE area is characterized by a complex hydrography, with sharp meridional gradients in temperature and salinity due to the convergence of the warm, saline KC and the cold, less saline OC (Fig. 2). Moreover, the KC transports warm seawater northward, where it cools and blends with the nutrient-rich OC (Wan et al., 2023; Xu et al., 2023). The resulting upward flux of nutrients induced by the mesoscale eddies from the Kuroshio and the Kuroshio Extension replenish the upper ocean in the KOE with a substantial nutrient supply

(Fig. S2). This, in turn, enhances primary productivity in the surface seawater, as 483 evidenced by the elevated Chl-a concentrations observed here (Fig. 2 and Fig. S2). 484 The higher surface seawater concentrations of CHCl₃ and C₂HCl₃ in the KOE 485 are likely attributable to a combination of factors, including phytoplankton activity, 486 terrestrial air mass transport, and physical conditions. Given the proximity of the 487 KOE region to land, atmospheric CHCl₃ and C₂HCl₃ might have been augmented 488 489 by inputs from long-distance land-based air masses originating from land (as discussed in Section 3.1). Additionally, the lower surface seawater temperature 490 491 (SST) in this region facilitated the dissolution of CHCl₃ and C₂HCl₃, while high atmospheric concentrations of these compounds from long-distance land transport 492 493 could have helped to replenish the CHCl₃ and C₂HCl₃ in the surface seawater. 494 However, the positive saturation anomalies of CHCl₃ and C₂HCl₃ were observed in the KOE (Fig. 4). In addition, elevated seawater concentrations of CHCl₃ and 495 C₂HCl₃, corresponding to high Chl-a concentrations in the KOE region (Fig. 2), 496 497 could be indicative of the influence of emissions from phytoplankton. Previous studies have demonstrated that phytoplankton blooms significantly contribute to 498 the production of these compounds (Abrahamsson et al., 1995; Abrahamsson et al., 499 2004b; Chuck et al., 2005; Roy et al., 2011; Lim et al., 2018). In particular, 500 501 diatoms and prymnesiophytes have been identified as dominant microalgal groups 502 releasing CHCl₃ (Roy et al., 2011; Lim et al., 2018). In the Northwest Pacific, diatoms and dinoflagellates are prevalent, with diatoms thriving in the 503 nutrient-rich Oyashio region (Wang et al., 2022), further supporting the biogenic 504 505 origin of CHCl₃ and C₂HCl₃ in this area. Taken together, the observed positive saturation anomalies (Fig. 4), together with the short atmospheric lifetimes of 506 these compounds (< 6 months; WMO, 2022), indicated that in situ phytoplankton 507

emissions exert a stronger control on seawater concentrations of CHCl₃ and C₂HCl₃ than terrestrial atmospheric inputs.

In contrast, CCl₄ and CH₃CCl₃ exhibited negative saturation anomalies in the KOE region (Fig. 4). Given that both gases are primarily of anthropogenic origin (Wang et al., 1995; Rigby et al., 2014), their elevated seawater concentrations in this region (Fig. 2) are likely attributable to long-range atmospheric transport from land. Moreover, the relatively low SST in the KOE might further enhance their solubility, reinforcing this undersaturation (Fig. 4). Collectively, these results highlight the dominant influence of atmospheric inputs in controlling the distribution of seawater of CCl₄ and CH₃CCl₃ in the KOE.

3.2.2 North Pacific Subtropical Gyre

In contrast to the KOE, the NPSG lies at the center of the subtropical gyre and is strongly influenced by a deep nutricline (Fig. 1a and Fig. 1b). It is characterized by high temperature and salinity but persistently low nutrient concentrations, as regional hydrographic conditions restrict the upward flux of nutrients through vertical transport (Xu et al., 2023; Fig. S2). Nutrient replenishment occurs primarily via vertical eddy diffusion, which is generally insufficient to sustain high productivity (Gupta et al., 2022). Consequently, the surface waters remain chronically nutrient-deficient, and the NPSG is often regarded as an oceanic desert with limited biological standing stocks. Figure 2 shows that concentrations of CHCl₃, C₂HCl₃, CCl₄, and CH₃CCl₃ in the NPSG were lower than in the KOE, likely because the NPSG is located far from land (Fig. 1a) and has a high SST (Fig. 2). Additionally, the Chl-a levels and nutrients were considerably lower in the NPSG than in the KOE region (Fig. S2). This suggested that the reduced release of CHCl₃ and C₂HCl₃ from phytoplankton could have also

contributed to the lower concentrations of these gases observed in the NPSG. Previous studies have confirmed that nutrient limitation reduces phytoplankton abundance, thereby lowering halocarbon production and emissions (Smythe-Wright et al., 2010; Liu et al., 2021).

3.2.3 Western Pacific Warm Pool

The WPWP is distinguished by strong stratification and a prominent barrier layer formed by heavy precipitation, which enhances surface-layer stability and restricts vertical nutrient transport (Qu and Meyers, 2005; Xu et al., 2023). Despite the abundance of subsurface nutrients, the presence of a shallow mixed layer and thick barrier layer limits nutrient exchange with the euphotic zone (Fig. S2). These conditions constrain primary productivity and, together with high SST, lead to relatively low surface seawater concentrations of CHCl₃ and C₂HCl₃, comparable to those observed in the NPSG (Fig. 2). However, seawater concentrations of CCl₄ and CH₃CCl₃ were relatively elevated near the equatorial WPWP (Fig. 2). This pattern likely reflected the proximity to landmasses such as Papua New Guinea, where terrestrial inputs via riverine runoff and atmospheric transport contribute to enhanced concentrations of these compounds in surface seawater (Fig. 1c).

3.2.4 Correlations between VCHCs in seawater

CHCl₃ and C₂HCl₃ were found to be supersaturated in seawater, with previous studies suggesting that they primarily originate from biological processes within the ocean rather than relying solely on atmospheric inputs (Section 3.2.1). The strong positive correlation between CHCl₃ and C₂HCl₃ in seawater (r = 0.71, p < 0.01, n = 65; Fig. S8) supported the idea that these compounds share a similar production mechanism, specifically emissions from biological processes. In contrast, CCl₄ and CH₃CCl₃ were undersaturated in seawater and primarily entered

the ocean through atmospheric deposition, meaning that their concentrations in seawater were more influenced by atmospheric inputs (Section 3.2.1). Moreover, despite the supersaturation of CHCl₃ and C₂HCl₃ in seawater and the undersaturation of CCl₄ and CH₃CCl₃, these four compounds still exhibited significant linear correlations in their concentrations (Fig. S8), suggesting that they were influenced by similar oceanic and atmospheric processes. This correlation likely reflected partially overlapping sources, such as riverine input and atmospheric transport (Fogelqvist, 1985; He et al., 2013a, 2013b). Additionally, oceanic physical processes, such as water mass mixing, diffusion, and vertical movement, played a crucial role in the distribution of gases in seawater (Doney et al., 2012). The synchronous influence of these processes on VCHCs might have been the reason for the linear correlation and similar distribution patterns observed for these four VCHCs in seawater. Specifically, in the Western Pacific, the unique hydrodynamic conditions significantly influenced the distribution patterns of CHCl₃, C₂HCl₃, CCl₄, and CH₃CCl₃. Major ocean currents, such as the Kuroshio and Oyashio, created zones of convergence and divergence that enhanced vertical and horizontal mixing, transporting gases from deeper waters to the surface and redistributing them across different regions, affecting their concentrations and distribution. Additionally, mesoscale eddies contribute to the diffusion of gases within the water column, resulting in gases from different sources (biogenic and atmospheric deposition) being more uniformly distributed in seawater (McGillicuddy Jr, 2016; Xu et al., 2023).

558

559

560

561

562

563

564

565

566

567

568

569

570

571

572

573

574

575

576

577

578

579

580

3.3 Sea-air fluxes and saturation anomalies of VCHCs

The saturation anomalies and sea-air fluxes of CHCl₃, C₂HCl₃, CCl₄, and CH₃CCl₃ were estimated based on their simultaneously measured seawater and

atmospheric concentrations, as outlined in Section 2.5 (Fig. 4 and Fig. 5). The saturation anomalies of CHCl₃ and C₂HCl₃ were positive, whereas CCl₄ and CH₃CCl₃ exhibited negative saturation anomalies at most stations of this study (Fig. 4). Moreover, the mean sea-air fluxes (range) for CHCl₃, C₂HCl₃, CCl₄, and CH₃CCl₃ were 23.96 (0.10–121.98), 7.18 (0.02–29.76), -0.73 (-3.44–0.00), and -0.02 (-0.18-0.07) nmol m⁻² d⁻¹. These results indicated that CHCl₃ and C₂HCl₃ were in a state of supersaturation in the surface seawater, leading to their emission into the overlying atmosphere. In contrast, CCl₄ and CH₃CCl₃ were undersaturated within the surface seawater and were assimilated from the overlying atmosphere. Hence, we tentatively concluded that the Western Pacific was a source of CHCl₃ and C₂HCl₃ and a sink for CCl₄ and CH₃CCl₃ during the cruise periods. Compared to the marginal sea of the Western Pacific, this study's estimates of CHCl₃ and C₂HCl₃ emission and CCl₄ and CH₃CCl₃ uptake were lower (Yang et al., 2015; He et al., 2017; Wei et al., 2019). For example, the average flux of CHCl₃ and C₂HCl₃ in this study was significantly lower than those reported in the northern Yellow Sea and Bohai Sea by He et al. (2017) (C₂HCl₃: 162.6 nmol m⁻² d⁻¹), Wei et al. (2019) (CHCl₃: 177.5 nmol m⁻² d⁻¹, C₂HCl₃: 99.5 nmol m⁻² d⁻¹), He et al. (2019) (C₂HCl₃: 59.4 nmol m⁻² d⁻¹), and Yang et al. (2015) (CHCl₃: 183.4 nmol m⁻² d⁻¹). Compared with the average fluxes of CCl₄ (-21.3 nmol m⁻² d⁻¹) and CH₃CCl₃ (-6.8 nmol m⁻² d⁻¹) in the South Yellow Sea and East China Sea as reported by Yang et al. (2015), the average fluxes of CCl₄ and CH₃CCl₃ in this study were lower. Although there were significant differences in sea-air fluxes compared with the marginal sea of the Western Pacific, both indicated that the

583

584

585

586

587

588

589

590

591

592

593

594

595

596

597

598

599

600

601

602

603

604

605

606

607

CH₃CCl₃.

ocean is a source of CHCl₃ and C₂HCl₃ in the atmosphere, but a sink of CCl₄ and

As shown in Fig. 5 and Fig. 6, the fluxes of CHCl₃ and C₂HCl₃ in the Western Pacific exhibited considerable spatial variability and generally corresponded with wind speeds. For instance, high fluxes of CHCl₃ and C₂HCl₃ at station P1-6 coincided with high wind speeds, while the low CHCl₃ and C₂HCl₃ fluxes at station E130-15 coincided with low wind speeds. However, as shown in Fig. 6, at a given wind speed, the fluxes were low due to low seawater concentrations of CHCl₃ and C₂HCl₃. Thus, seawater concentrations also had a large influence on the spatial variability of the sea-air fluxes of CHCl₃ and C₂HCl₃. The air-sea fluxes of CCl₄ and CH₃CCl₃ were also higher at stations with high wind speeds (Fig. 5 and Fig. 6). Similarly, Butler et al. (2016) found that the air-sea exchange rate was the primary driver of oceanic uptake of CCl4, mainly driven by wind speed. However, the highest air-sea fluxes of CCl₄ and CH₃CCl₃ were observed at station P1-2, which had the highest equilibrium solubility (ratio of atmospheric concentration to Henry's Law constant) (Fig. 5). Moreover, at a given wind speed, the fluxes of CCl₄ and CH₃CCl₃ were lower where their atmospheric concentrations were lower and where SST was higher (Fig. 6). Therefore, the spatial variability of sea-air CCl₄ and CH₃CCl₃ fluxes were not only affected by wind speed but were also related to atmospheric CCl₄ and CH₃CCl₃ concentrations and SST. A similar investigation observed a comparable relationship between sea-air fluxes, wind speed, and atmospheric concentration while examining the distribution of SF₆ in seawater (Ni et al., 2023). It should be noted that the sea-air flux estimates of CHCl₃, C₂HCl₃, CCl₄, and CH₃CCl₃ presented in this study are derived exclusively from autumn and winter

608

609

610

611

612

613

614

615

616

617

618

619

620

621

622

623

624

625

626

627

628

629

630

631

632

cruise observations, and thus may not fully represent their annual averages due to

seasonal variability. The spatiotemporal patterns of sea-air fluxes are primarily

governed by the concentrations of VCHCs in the atmosphere and seawater, SST, and wind speed. In particular, seawater concentrations of CHCl₃ and C₂HCl₃ are strongly modulated by biological activity (Section 3.2), while both SST and wind speed exhibit pronounced seasonal variations (Fig. 7a). Moreover, according to AGAGE data (https://agage.mit.edu/), the interannual variability of global atmospheric CCl₄ in 2019 was 2%, with variability at GSN sites of 3% (Fig. 7b), whereas global atmospheric CH₃CCl₃ varied by 13% (Fig. 7c). During the observation period (October-December 2019), mean atmospheric concentrations at both GSN sites and the global scale were approximately 1% lower than their respective annual means, while the global CH₃CCl₃ concentration was about 6% lower (Fig. 7c). These results suggest that atmospheric CCl₄ levels in the Western Pacific were likely close to the annual mean during this period, whereas CH₃CCl₃ levels were possibly somewhat lower. In addition, SST and Chl-a in the study region during the observation period were broadly consistent with their annual means, whereas wind speeds were on average 6% higher (Fig. 7a; Tang et al., 2022). Consequently, the sea-air fluxes of CHCl₃, C₂HCl₃, and CCl₄ reported in this study are likely somewhat higher than the annual mean, primarily due to the elevated wind speeds during the cruises. In the Western Pacific (130°E–180°E, 0°–40°N, area: 2.17×10^7 km²), the

633

634

635

636

637

638

639

640

641

642

643

644

645

646

647

648

649

650

651

652

653

654

655

656

657

In the Western Pacific (130°E–180°E, 0°–40°N, area: 2.17 × 10⁷ km²), the estimated annual oceanic uptake of CCl₄ was 0.9 Gg yr⁻¹. The associated uncertainty was quantified by combining the 95% confidence interval, derived from the standard error of fluxes within the study region, with the inherent >20% systematic uncertainty of flux estimates. The resulting uptake range is 0.5–1.3 Gg yr⁻¹, with an overall uncertainty of 0.4 Gg yr⁻¹. Given that fluxes during the observation period were likely higher than annual averages, the annual CCl₄

uptake estimated in this study may be slightly overestimated. Moreover, considering that elevated SST reduces gas solubility, strengthens ocean stratification, and alters wind patterns, future warming of the western Pacific is expected to diminish the oceanic sink capacity for CCl₄.

3.4 The role of the Western Pacific in regulating Eastern Asia CCl₄

658

659

660

661

662

663

664

665

666

667

668

669

670

671

672

673

674

675

676

677

678

679

680

681

682

Eastern Asia, particularly eastern China, was a major source of global CCl₄ emissions, significantly contributing to the global CCl₄ burden (Lunt et al., 2018). The primary emission sources included the manufacture of general-purpose machinery, the production of CH₃Cl, CH₂Cl₂, CHCl₃, and C₂Cl₄, which generate CCl₄ as a byproduct, as well as the use of CCl₄ as a raw material and processing agent in the chemical manufacturing industry (Park et al., 2018; Li et al., 2024). Although CCl₄ emissions from eastern China declined significantly by nearly 45% between 2016 and 2019, Eastern Asia remained a major source of atmospheric CCl₄ (WMO, 2022). Our study suggested that CCl₄ emissions from Eastern Asia may have been a significant source of atmospheric CCl₄ in the Western Pacific (Section 3.1). The Western Pacific, as a sink for East Asian CCl₄, played a key role in regulating atmospheric CCl₄ concentrations. Based on our estimates (Section 3.3), the estimated oceanic absorption of CCl₄ in the Western Pacific (0.9 \pm 0.4 Gg vr^{-1}) accounted for $14.3 \pm 6.8\%$ of the Eastern China emissions $(6.3 \pm 1.1 \text{ Gg yr}^{-1})$ in 2019; WMO, 2022), $5.6 \pm 2.5\%$ of the emissions from Eastern Asia (16 (9–24) Gg yr⁻¹ on average between 2009 and 2016; Lunt et al., 2018), and $2.1 \pm 1.1\%$ of the total global emissions (global emissions were 44 ± 14 Gg yr⁻¹; WMO, 2022). Furthermore, the estimated oceanic absorption of CCl₄ in the Western Pacific accounted for $6.3 \pm 2.8\%$ of the global oceanic absorption (14.4 Gg yr⁻¹; Butler et al., 2016). These data indicated that the Western Pacific as a sink of CCl₄ was

crucial for regulating atmospheric CCl₄ concentrations and mitigating the accumulation of CCl₄ in the atmosphere of Eastern Asia. This result was consistent with Butler et al. (2016), further confirming the critical role of the Western Pacific in the global CCl₄ cycle and emphasizing the ocean's indispensable role as a sink for atmospheric CCl₄. Notably, despite the estimate originating from a region with relatively little anthropogenic influence, the absorption capacity of the Western Pacific indicates it can significantly contribute to reducing global CCl₄ levels. This finding also aligned with Yvon-Lewis and Butler (2002), who demonstrated that oceans could effectively remove substantial quantities of CCl₄ from the atmosphere.

Additionally, a substantial body of prior data has indicated there is a CCl4 deficit in deep ocean waters, especially in regions characterized by low oxygen levels (Krysell et al., 1994; Tanhua and Olsson, 2005). Recent studies have observed widespread undersaturation of CCl4 in the surface waters of the Pacific, Atlantic, and Southern Oceans, suggesting the oceans consume a substantial amount of atmospheric CCl4 and that biological sinks for CCl4 may exist in the surface or near-surface waters of the oceans (Butler et al., 2016; Suntharalingam et al., 2019). These findings further supported the role of oceans as a CCl4 sink and provided important insights for future oceanic environmental management and pollution control.

4 Conclusions

This study investigated the seawater and atmospheric concentrations, sea-air fluxes, sources, and control factors of VCHCs in the Western Pacific during October 2019 and January 2020. As summarized from Figure 8, the presence or absence of upwelling, whether the upwelling carries nutrients, and the transport of

terrestrial inputs govern the biogeochemical characteristics of surface seawater in the Western Pacific, thereby influencing the concentrations and distributions of climatically relevant VCHCs. Specifically, the mesoscale eddies in the KOE region induced upwelling, bringing nutrient-rich subsurface water to the surface. This upwelling supplied ample nutrients to the surface seawater, enhancing phytoplankton growth and organic matter photoreactions. These processes potentially enhanced the production of CHCl₃ and C₂HCl₃, resulting in high seawater concentrations of these compounds in the KOE. In contrast, the lower seawater concentrations of CHCl₃ and C₂HCl₃ in the NPSG and WPWP were attributed to the oligotrophic subsurface seawater in the NPSG and the suppression of upward nutrient and organic matter fluxes due to a robust barrier layer in the WPWP. The elevated seawater concentrations of CCl₄ and CH₃CCl₃ observed in the coastal area were caused by atmospheric inputs, seawater temperatures, and upwelling. Atmospheric mixing ratios of CCl₄ and CH₃CCl₃ over the Western Pacific were predominantly determined by atmospheric inputs from land, as revealed through backward trajectory analysis. However, the atmospheric concentration of CHCl₃ and C₂HCl₃ in the study area was likely influenced by a combination of atmospheric transport from the continent and ocean emissions, with continental air mass transport potentially contributing more significantly. The preliminary estimation indicated that approximately 2.2 ± 1.1% of global CCl₄ emissions were absorbed by the Western Pacific. Our study also showed that 14.3 \pm 6.8% of CCl₄ emitted from Eastern China and 5.6 \pm 2.5% of Eastern Asia CCl₄ emissions could be absorbed by the Western Pacific, highlighting its crucial role in regulating atmospheric CCl₄ concentrations and mitigating accumulation in the Eastern Asia atmosphere. In light of these findings, we tentatively propose that the

708

709

710

711

712

713

714

715

716

717

718

719

720

721

722

723

724

725

726

727

728

729

730

731

capacity of the ocean to act as a sink for CCl₄ may warrant reevaluation. The global oceanic uptake of CCl₄ and CH₃CCl₃ and emissions of CHCl₃ and C₂HCl₃ could have an influence on their global abundances and impact atmospheric chemistry. Future studies should prioritize expanded temporal and spatial observations to better constrain these processes and improve climate predictions.

Acknowledgments

We thank the chief scientists, captains, and crews of the R/V "Science" and "Dongfanghong 3" for their assistance and cooperation during the investigation. This work was funded by the National Natural Science Foundation of China (grant numbers 42276039 and 42406040), Taishan Scholars Project Special Fund Support (tspd 20240805), Postdoctoral Fellowship Program of CPSF (GZC20232705), Shandong Provincial Postdoctoral Foundation Project (Innovation Project) (SDCX-ZG-202400181), and the Qingdao Postdoctoral Applied Research Project (QDBSH20240101018). We thank the Institute of Oceanology, CAS, for samples and data from the NORC2019-09 cruise (NSFC grant 41849909) and the First Institute of Oceanography, MNR, for Chl-*a* data, with special thanks to Honghai Zhang of Ocean University of China for Chl-*a* data.

Data availability statement

The datasets are accessible via Figshare at https://doi.org/ 752 10.6084/m9.figshare.25639146.

Author contributions:

SL and JN designed the study, conducted VCHC measurements in the Western Pacific, analyzed the results, and contributed to manuscript writing. XG assisted with the observations. JS reviewed and revised the manuscript. ZH interpreted the data and contributed to the manuscript. GY interpreted the analyzed

- results and reviewed and revised the manuscript.
- 759 Competing interests
- The authors declare that they have no conflict of interest.
- 761 References
- 762 References
- Abrahamsson, K., Bertilsson, S., Chierici, M., Fransson, A., Froneman, P. W.,
- Lorén, A., & Pakhomov, E. A. (2004a). Variations of biochemical parameters
- along a transect in the Southern Ocean, with special emphasis on volatile
- halogenated organic compounds. Deep Sea Research Part II: Topical Studies
- 767 in Oceanography, 51(22-24), 2745-2756.
- Abrahamsson, K., Ekdahl, A., Collen, J., & Pedersen, M. (1995). Marine algae
- source of trichloroethylene and perchloroethylene. Limnology and
- 770 Oceanography, 40(7), 1321-1326.
- Abrahamsson, K., & Ekdahl, A. (1996). Volatile halogenated compounds and
- chlorophenols in the Skagerrak. Journal of Sea Research, 35(1-3), 73-79.
- Abrahamsson, K., Lorén, A., Wulff, A., & Wängberg, S. Å. (2004b). Air-sea
- exchange of halocarbons: the influence of diurnal and regional variations and
- distribution of pigments. Deep Sea Research Part II: Topical Studies in
- 776 Oceanography, 51(22-24), 2789-2805.
- An, M., Western, L. M., Say, D., Chen, L., Claxton, T., Ganesan, A. L., et al.
- 778 (2021). Rapid increase in dichloromethane emissions from China inferred
- through atmospheric observations. Nature Communications, 12(1), 7279.
- 780 An, M., Western, L. M., Hu, J., Yao, B., Mühle, J., Ganesan, A. L., et al. (2023).
- Anthropogenic chloroform emissions from China drive changes in global
- 782 emissions. Environmental Science & Technology, 57(37), 13925-13936.

- 783 Blake, N. J., Blake, D. R., Simpson, I. J., Meinardi, S., Swanson, A. L., Lopez, J.
- P., et al. (2003). NMHCs and halocarbons in Asian continental outflow
- during the Transport and Chemical Evolution over the Pacific (TRACE-P)
- Field Campaign: Comparison with PEM-West B. Journal of Geophysical
- 787 Research: Atmospheres, 108(D20).
- 788 Bravo-Linares, C. M., Mudge, S. M., & Loyola-Sepulveda, R. H. (2007).
- Occurrence of volatile organic compounds (VOCs) in Liverpool Bay, Irish
- 790 Sea. Marine Pollution Bulletin, 54(11), 1742-1753.
- Butler, J. H., Yvon-Lewis, S. A., Lobert, J. M., King, D. B., Montzka, S. A.,
- Bullister, J. L., et al. (2016). A comprehensive estimate for loss of
- atmospheric carbon tetrachloride (CCl₄) to the ocean. Atmospheric Chemistry
- 794 and Physics, 16(17), 10899-10910.
- Byčenkienė, S., Dudoitis, V., & Ulevicius, V. (2014). The use of trajectory cluster
- analysis to evaluate the long-range transport of black carbon aerosol in the
- south-eastern Baltic region. Advances in Meteorology, 2014.
- 798 Carpenter, L. J., Reimann, S., Burkholder, J. B., Clerbaux, C., Hall, B. D.,
- Hossaini, R., et al. (2014). Update on ozone-depleting substances (ODSs) and
- other gases of interest to the Montreal protocol. 9789966076014.
- 801 Chang, C. Y., Wang, J. L, Chen, Y. C., Pan, X. X., Chen, W. N., Lin, M. R., et al.
- 802 (2022). A study of the vertical homogeneity of trace gases in East Asian
- continental outflow. Chemosphere, 297, 134165.
- 804 Chipperfield, M. P., Hossaini, R., Montzka, S. A., Reimann, S., Sherry, D., &
- 805 Tegtmeier, S. (2020). Renewed and emerging concerns over the production
- and emission of ozone-depleting substances. Nature Reviews Earth &
- 807 Environment, 1(5), 251-263.

- 808 Christof, O., Seifert, R., & Michaelis, W. (2002). Volatile halogenated organic
- compounds in European estuaries. Biogeochemistry, 59, 143-160.
- 810 Chuck, A. L., Turner, S. M., & Liss, P. S. (2005). Oceanic distributions and air-sea
- fluxes of biogenic halocarbons in the open ocean. Journal of Geophysical
- Research: Oceans, 110(C10).
- Doney, S. C., Ruckelshaus, M., Emmett Duffy, J., Barry, J. P., Chan, F., English, C.
- A., et al. (2012). Climate change impacts on marine ecosystems. Annual
- Review of Marine Science, 4(1), 11-37.
- 816 Ekdahl, A., Pedersén, M., & Abrahamsson, K. (1998). A study of the diurnal
- variation of biogenic volatile halocarbons. Marine Chemistry, 63(1-2), 1-8.
- 818 Fang, X., Park, S., Saito, T., Tunnicliffe, R., Ganesan, A. L., Rigby, M., et al.
- 819 (2019). Rapid increase in ozone-depleting chloroform emissions from China.
- 820 Nature Geoscience, 12(2), 89-93.
- 821 Fogelqvist, E. (1985). Carbon tetrachloride, tetrachloroethylene, 1, 1,
- 822 1-trichloroethane and bromoform in Arctic seawater. Journal of Geophysical
- 823 Research: Oceans, 90(C5), 9181-9193.
- 624 Gschwend, P. M., MacFarlane, J. K., & Newman, K. A. (1985). Volatile
- halogenated organic compounds released to seawater from temperate marine
- macroalgae. Science, 227(4690), 1033-1035.
- Gossett, J. M. (1987). Measurement of Henry's law constants for C1 and C2
- chlorinated hydrocarbons. Environmental Science & Technology, 21(2),
- 829 202-208.
- 630 Gupta, M., Williams, R. G., Lauderdale, J. M., Jahn, O., Hill, C., Dutkiewicz, S.,
- & Follows, M. J. (2022). A nutrient relay sustains subtropical ocean

- productivity. Proceedings of the National Academy of Sciences, 119(41),
- 833 e2206504119.
- 834 He, Z., Liu, S. S., Ni, J., Chen, Y., & Yang, G. P. (2019). Spatio-temporal
- variability and sources of volatile halocarbons in the South Yellow Sea and
- the East China Sea. Marine Pollution Bulletin, 149, 110583.
- He, Z., Yang, G. P., & Lu, X. L. (2013a). Distributions and sea-to-air fluxes of
- volatile halocarbons in the East China Sea in early winter. Chemosphere,
- 839 90(2), 747-757.
- He, Z., Liu, Q. L., Zhang, Y. J., & Yang, G. P. (2017). Distribution and sea-to-air
- fluxes of volatile halocarbons in the Bohai Sea and North Yellow Sea during
- spring. Science of the Total Environment, 585, 546-553.
- He, Z., Yang, G., Lu, X., & Zhang, H. (2013b). Distributions and sea-to-air fluxes
- of chloroform, trichloroethylene, tetrachloroethylene, chlorodibromomethane
- and bromoform in the Yellow Sea and the East China Sea during spring.
- Environmental Pollution, 177, 28-37.
- 847 He, Z., Yang, G. P., Lu, X. L., Ding, Q. Y., & Zhang, H. H. (2013c). Halocarbons
- in the marine atmosphere and surface seawater of the south Yellow Sea
- during spring. Atmospheric Environment, 80, 514-523.
- Hersbach, H., Bell, B., Berrisford, P., Hirahara, S., Horányi, A., Muñoz-Sabater, J.,
- et al. (2020). The ERA5 global reanalysis. Quarterly Journal of the Royal
- Meteorological Society, 146(730), 1999-2049.
- Hossaini, R., Chipperfield, M. P., Saiz-Lopez, A., Harrison, J. J., von Glasow, R.,
- Sommariva, R., et al. (2015). Growth in stratospheric chlorine from
- short-lived chemicals not controlled by the Montreal Protocol. Geophysical
- Research Letters, 42(11), 4573-4580.

- Hossaini, R., Chipperfield, M. P., Montzka, S. A., Leeson, A. A., Dhomse, S. S., &
- Pyle, J. A. (2017). The increasing threat to stratospheric ozone from
- dichloromethane. Nature Communications, 8(1), 15962.
- Hu, D., Wang, F., Sprintall, J., Wu, L., Riser, S., Cravatte, S., et al. (2020). Review
- on observational studies of western tropical Pacific Ocean circulation and
- climate. Journal of Oceanology and Limnology, 38(4), 906-929.
- 863 Hu, D., Wu, L., Cai, W., Gupta, A. S., Ganachaud, A., Qiu, B., et al. (2015).
- Pacific western boundary currents and their roles in climate. Nature,
- 865 522(7556), 299-308.
- Hunter-Smith, R. J, Balls, P. W., & Liss, P. S (1983). Henry's law constants and the
- air-sea exchange of various low molecular weight halocarbon gases. Tellus B:
- Chemical and Physical Meteorology, 35(3), 170-176.
- 869 Jiao, Y., Ruecker, A., Deventer, M. J., Chow, A. T., & Rhew, R. C. (2018).
- Halocarbon emissions from a degraded forested wetland in coastal South
- Carolina impacted by sea level rise. ACS Earth and Space Chemistry, 2(10),
- 955-967.
- 873 Karlsson, A., Auer, N., Schulz-Bull, D., & Abrahamsson, K. (2008).
- Cyanobacterial blooms in the Baltic-A source of halocarbons. Marine
- 875 Chemistry, 110(3-4), 129-139.
- Khalil, M. A. K., Moore, R. M., Harper, D. B., Lobert, J. M., Erickson, D. J.,
- Koropalov, V., et al. (1999). Natural emissions of chlorine-containing gases:
- Reactive Chlorine Emissions Inventory. Journal of Geophysical Research:
- 879 Atmospheres, 104(D7), 8333-8346.
- 880 Khan, M. A. H., Rhew, R. C., Whelan, M. E., Zhou, K., & Deverel, S. J. (2011).
- Methyl halide and chloroform emissions from a subsiding Sacramento-San

- Joaquin Delta island converted to rice fields. Atmospheric Environment,
- 883 45(4), 977-985.
- Krysell, M., Fogelqvist, E., & Tanhua, T. (1994). Apparent removal of the transient
- 885 tracer carbon tetrachloride from anoxic seawater. Geophysical Research
- 886 Letters, 21(23), 2511-2514.
- Kurihara, M. K., Kimura, M., Iwamoto, Y., Narita, Y., Ooki, A., Eum, Y J., et al.
- 888 (2010). Distributions of short-lived iodocarbons and biogenic trace gases in
- the open ocean and atmosphere in the western North Pacific. Marine
- 890 Chemistry, 118, 156-170.
- 891 Li, B., Huang, J., Hu, X., Zhang, L., Ma, M., Hu, L., et al. (2024). CCl₄ emissions
- in eastern China during 2021–2022 and exploration of potential new sources.
- Nature Communications, 15(1), 1725.
- 894 Li, J. L., Zhai, X., Ma, Z., Zhang, H. H., & Yang, G. P. (2019). Spatial
- distributions and sea-to-air fluxes of non-methane hydrocarbons in the
- atmosphere and seawater of the Western Pacific. Science of the Total
- 897 Environment, 672, 491-501.
- Liang, Q., Jaeglé, L., Jaffe, D. A., Weiss-Penzias, P., Heckman, A., & Snow, J. A.
- 899 (2004). Long-range transport of Asian pollution to the northeast Pacific:
- 900 Seasonal variations and transport pathways of carbon monoxide. Journal of
- Geophysical Research: Atmospheres, 109(D23).
- Liang, Q., Newman, P. A., Daniel, J. S., Reimann, S., Hall, B. D., Dutton, G., &
- 803 Kuijpers, L. J. (2014). Constraining the carbon tetrachloride (CCl₄) budget
- using its global trend and inter-hemispheric gradient. Geophysical Research
- 905 Letters, 41(14), 5307-5315.
- Liang, Q., Newman, P. A., & Reimann, S. (2016). SPARC report on the mystery of

- carbon tetrachloride. ETH Zurich, SPARC, Volume 7.
- 908 Lim, Y. K., Phang, S. M., Sturges, W. T., Malin, G., & Rahman, N. B. A. (2018).
- 909 Emission of short-lived halocarbons by three common tropical marine
- microalgae during batch culture. Journal of Applied Phycolpgy, 30(1), 1-13.
- Liu, T., Gong, S., He, J., Yu, M., Wang, Q., Li, H., et al. (2017). Attributions of
- meteorological and emission factors to the 2015 winter severe haze pollution
- episodes in China's Jing-Jin-Ji area. Atmospheric Chemistry and Physics,
- 914 17(4), 2971-2980.
- 915 Liu, S. S., Yang, G. P., He, Z., Gao, X. X., & Xu, F. (2021). Oceanic emissions of
- methyl halides and effect of nutrients concentration on their production: A case
- of the Northwest Pacific (2°N to 24°N). Science of the Total Environment, 769,
- 918 144488.
- 919 Lunt, M. F., Park, S., Li, S., Henne, S., Manning, A. J., Ganesan, A. L., et al.
- 920 (2018). Continued emissions of the ozone-depleting substance carbon
- 921 tetrachloride from Eastern Asia. Geophysical Research Letters, 45(20),
- 922 11-423.
- 923 McCulloch, A. (2003). Chloroform in the environment: occurrence, sources, sinks
- 924 and effects. Chemosphere, 50(10), 1291-1308.
- 925 McGillicuddy Jr, D. J. (2016). Mechanisms of physical-biological-biogeochemical
- interaction at the oceanic mesoscale. Annual Review of Marine Science, 8(1),
- 927 125-159.
- Menemenlis, D., Campin, J. M., Heimbach, P., Hill, C., Lee, T., Nguyen, A., et al.
- 929 (2008). ECCO2: High resolution global ocean and sea ice data synthesis.
- 930 Mercator Ocean Quarterly Newsletter, 31, 13-21.
- 931 Montzka, S. A., Reimann, S., Engel, A., Krüger, K., O'Doherty, S., Sturges, W. T.,

- et al. (2011). Ozone depleting substances (ODS's) and related chemicals,
- Chapter 1 in: scientific assessment of Ozone Depletion: 2010. Global Ozone
- Research and Monitoring Project. World Meteorological Organization,
- 935 Geneva, Switzerland, 516, 1-112.
- Moore, R. M. (2000). The solubility of a suite of low molecular weight
- organochlorine compounds in seawater and implications for estimating the
- marine source of methyl chloride to the atmosphere. Chemosphere-Global
- 939 Change Science, 2(1), 95-99.
- 940 Moore, R. M. (2003). Marine sources of volatile organohalogens. Natural
- Production of Organohalogen Compounds, 85-101.
- 942 NASA Ocean Biology Processing Group. (2022). Aqua MODIS Level 3 Mapped
- 943 Chlorophyll Data, Version R2022.0 [dataset]. NASA Ocean Biology
- 944 Distributed Active Archive Center.
- Ni, J., Liu, S. S., Lang, X. P., He, Z., & Yang, G. P. (2023). Sulfur hexafluoride in
- the marine atmosphere and surface seawater of the Western Pacific and
- Eastern Indian Ocean. Environmental Pollution, 335, 122266.
- Oram, D. E., Ashfold, M. J., Laube, J. C., Gooch, L. J., Humphrey, S., Sturges, W.
- T., et al. (2017). A growing threat to the ozone layer from short-lived
- anthropogenic chlorocarbons. Atmospheric Chemistry and Physics, 17(19),
- 951 11929-11941.
- 952 Ou-Yang, C. F., Chang, C. C., Wang, J. L., Shimada, K., Hatakeyama, S., Kato, S.,
- et al. (2017). Characteristics of summertime volatile organic compounds in
- the lower free troposphere: Background measurements at Mt. Fuji. Aerosol
- 955 and Air Quality Research, 17(12), 3037-3051.
- 956 Park, S., Li, S., Mühle, J., O'Doherty, S., Weiss, R. F., Fang, X., et al. (2018).

- Toward resolving the budget discrepancy of ozone-depleting carbon
- 958 tetrachloride (CCl₄): an analysis of top-down emissions from China.
- 959 Atmospheric Chemistry and Physics, 18(16), 11729-11738.
- 960 Plummer, J. D., & Edzwald, J. K. (2002). Effects of chlorine and ozone on algal
- cell properties and removal of algae by coagulation. Journal of Water Supply:
- Research and Technology-AQUA, 51(6), 307-318.
- 963 Qu, T., & Meyers, G. (2005). Seasonal variation of barrier layer in the
- southeastern tropical Indian Ocean. Journal of Geophysical Research: Oceans,
- 965 110(C11).
- Quack, B., & Suess, E. (1999). Volatile halogenated hydrocarbons over the
- 967 western Pacific between 43°N and 4°N. Journal of Geophysical Research:
- 968 Atmospheres, 104(D1), 1663-1678.
- Rigby, M., Prinn, R. G., O'doherty, S., Miller, B. R., Ivy, D., Mühle, J., et al.
- 970 (2014). Recent and future trends in synthetic greenhouse gas radiative forcing.
- Geophysical Research Letters, 41(7), 2623-2630.
- 872 Roy, R., Pratihary, A., Narvenkar, G., Mochemadkar, S., Gauns, M., & Nagyi, S.
- W. A. (2011). The relationship between volatile halocarbons and
- 974 phytoplankton pigments during a Trichodesmium bloom in the coastal eastern
- 975 Arabian Sea. Estuarine, Coastal and Shelf Science, 95(1), 110-118.
- 976 Saiz-Lopez, A., Fernandez, R. P., Li, Q., Cuevas, C. A., Fu, X., Kinnison, D. E., et
- al. (2023). Natural short-lived halogens exert an indirect cooling effect on the
- 978 climate. Nature, 618(7967), 967-973.
- Say, D., Kuyper, B., Western, L., Khan, M. A. H., Lesch, T., Labuschagne, C., et al.
- 980 (2020). Emissions and marine boundary layer concentrations of unregulated
- chlorocarbons measured at Cape Point, South Africa. Environmental Science

- 982 & Technology, 54(17), 10514-10523.
- 983 Scarratt, M. G., & Moore, R. M. (1999). Production of chlorinated hydrocarbons
- and methyl iodide by the red microalga Porphyridium purpureum. Limnology
- 985 and Oceanography, 44(3), 703-707.
- Schwardt, A., Dahmke, A., & Köber, R. (2021). Henry's law constants of volatile
- organic compounds between 0 and 95 °C-Data compilation and
- complementation in context of urban temperature increases of the subsurface.
- 989 Chemosphere, 272, 129858.
- 990 Shechner, M., Guenther, A., Rhew, R., Wishkerman, A., Li, Q., Blake, D., et al.
- 991 (2019). Emission of volatile halogenated organic compounds over various
- 992 Dead Sea landscapes. Atmospheric Chemistry and Physics, 19(11),
- 993 7667-7690.
- 994 Sherry, D., McCulloch, A., Liang, Q., Reimann, S., & Newman, P. A. (2018).
- 995 Current sources of carbon tetrachloride (CCl₄) in our atmosphere.
- Environmental Research Letters, 13(2), 024004.
- 997 Shi, J., Jia, Q., Nürnberg, D., Li, T., Xiong, Z., & Qin, B. (2022). Coupled
- nutricline and productivity variations during the Pliocene in the western
- Pacific warm pool and their paleoceanographic implications. Global and
- 1000 Planetary Change, 212, 103810.
- 1001 Shoemaker, D. P., Garland, G. W., & Steinfeld, J. I. (1974). Propagation of errors,
- 1002 3rd ed., McGraw-Hill: New York, pp 51-58.
- 1003 Squizzato, S., & Masiol, M. (2015). Application of meteorology-based methods to
- determine local and external contributions to particulate matter pollution: A
- case study in Venice (Italy). Atmospheric Environment, 119, 69-81.

- Smythe-Wright, D., Peckett, C., Boswell, S., & Harrison, R. (2010). Controls on
- the production of organohalogens by phytoplankton: Effect of nitrate
- concentration and grazing. Journal of Geophysical Research: Biogeosciences,
- 1009 115(G3).
- 1010 Stohl, A., Eckhardt, S., Forster, C., James, P., & Spichtinger, N. (2002). On the
- pathways and timescales of intercontinental air pollution transport. Journal of
- 1012 Geophysical Research: Atmospheres, 107(D23), ACH-6.
- 1013 Suntharalingam, P., Buitenhuis, E., Carpenter, L. J., Butler, J. H., Messias, M. J.,
- Andrews, S. J., & Hackenberg, S. C. (2019). Evaluating oceanic uptake of
- atmospheric CCl₄: A combined analysis of model simulations and
- observations. Geophysical Research Letters, 46(1), 472-482.
- 1017 Tanhua, T., & Olsson, K. A. (2005). Removal and bioaccumulation of
- anthropogenic, halogenated transient tracers in an anoxic fjord. Marine
- 1019 Chemistry, 94(1-4), 27-41.
- 1020 Tang, C., Tao, X., Wei, Y., Tong, Z., Zhu, F., & Lin, H. (2022). Analysis and
- prediction of wind speed effects in East Asia and the Western Pacific based
- on multi-source data. Sustainability, 14(19), 12089.
- 1023 Tsunogai, S. (2002). The western North Pacific playing a key role in global
- biogeochemical fluxes. Journal of Oceanography, 58, 245-257.
- 1025 US EPA. (2019). Method TO-15A: Determination of volatile organic compounds
- 1026 (VOCs) in air collected in specially prepared canisters and analyzed by gas
- 1027 chromatography—mass spectrometry (GC-MS).
- https://nepis.epa.gov/Exe/ZyNET.exe/P100YDPO.TXT?ZyActionD=ZyDocume
- nt&Client=EPA&Index=2016+Thru+2020&Docs=&Quer

- 1030 Wan, S., Xiang, R., Steinke, S., Du, Y., Yang, Y., Wang, S., & Wang, H. (2023).
- 1031 Impact of the Western Pacific Warm pool and Kuroshio dynamics in the
- Okinawa Trough during the Holocene. Global and Planetary Change, 224,
- 1033 104116.
- Wang, J. L., Blake, D. R., & Rowland, F. S. (1995). Seasonal variations in the
- atmospheric distribution of a reactive chlorine compound, tetrachloroethene
- 1036 (CCl₂=CCl₂). Geophysical Research Letters, 22(9), 1097-1100.
- Wang, B., Kang, I. S., & Lee, J. Y. (2004). Ensemble simulations of
- 1038 Asian–Australian monsoon variability by 11 AGCMs. Journal of Climate,
- 1039 17(4), 803-818.
- 1040 Wang, Y., Bi, R., Zhang, J., Gao, J., Takeda, S., Kondo, Y., et al. (2022).
- 1041 Phytoplankton distributions in the Kuroshio-Oyashio Region of the
- Northwest Pacific Ocean: Implications for marine ecology and carbon cycle.
- Frontiers in Marine Science, 9, 865142.
- Wanninkhof, R. (2014). Relationship between wind speed and gas exchange over
- the ocean revisited. Limnology & Oceanography: Methods, 12, 351-362.
- 1046 Wei, Y., He, Z., & Yang, G. P. (2019). Seasonal and spatial variations of
- 1047 chloroform, trichloroethylene, tetrachloroethylene, chlorodibromomethane,
- and bromoform in the Northern Yellow Sea and Bohai Sea. Environmental
- 1049 Chemistry, 16(2), 114-124.
- 1050 WMO (World Meteorological Organization). (2007). Scientific Assessment of
- Ozone Depletion: 2006, Global Ozone Research and Monitoring
- Project-Report No. 50, 572 pp., Geneva, Switzerland.
- 1053 WMO (World Meteorological Organization). (2022). Scientific Assessment of
- Ozone Depletion 2022. Global Ozone Research and Monitoring

- 1055 Project-Report No. 278, 509 pp, Geneva, Switzerland.
- 1056 Xu, F., Zhang, H. H., Yan, S. B., Sun, M. X., Wu, J. W., & Yang, G. P. (2023).
- Biogeochemical controls on climatically active gases and atmospheric sulfate
- aerosols in the western Pacific. Environmental Research, 220, 115211.
- 1059 Yang, G. P., Li, L., Lu, X. L., & Zhang, L. (2015). Distributions and sea-to-air
- fluxes of volatile halocarbons in the southern Yellow Sea and the East China
- Sea. Acta Oceanologica Sinica, 34(2), 9-20.
- 1062 Yi, L., An, M., Yu, H., Ma, Z., Xu, L., O'Doherty, S., et al. (2023). In Situ
- Observations of Halogenated Gases at the Shangdianzi Background Station
- and Emission Estimates for Northern China. Environmental Science &
- Technology, 57(18), 7217-7229.
- 1066 Yi, L., Wu, J., An, M., Xu, W., Fang, X., Yao, B., et al. (2021). The atmospheric
- concentrations and emissions of major halocarbons in China during 2009–2019.
- Environmental Pollution, 284, 117190.
- 1069 Yokouchi, Y., Inagaki, T., Yazawa, K., Tamaru, T., Enomoto, T., & Izumi, K.
- 1070 (2005). Estimates of ratios of anthropogenic halocarbon emissions from
- Japan based on aircraft monitoring over Sagami Bay, Japan. Journal of
- Geophysical Research: Atmospheres, 110(D6).
- 1073 Yokouchi, Y., Li, H. J., Machida, T., Aoki, S., & Akimoto, H. (1999). Isoprene in the
- marine boundary layer (Southeast Asian Sea, eastern Indian Ocean, and Southern
- Ocean): Comparison with dimethyl sulfide and bromoform. Journal of
- Geophysical Research: Atmospheres, 104(D7), 8067-8076.
- 1077 Yokouchi, Y., Inoue, J., & Toom-Sauntry, D. (2013). Distribution of natural
- halocarbons in marine boundary air over the Arctic Ocean. Geophysical
- 1079 Research Letters, 40, 4086–4091.

- 1080 Yu, D., Yao, B., Lin, W., Vollmer, M. K., Ge, B., Zhang, G., et al. (2020).
- 1081 Atmospheric CH₃CCl₃ observations in China: Historical trends and
- implications. Atmospheric Research, 231, 104658.
- 1083 Yvon-Lewis, S. A., & Butler, J. H. (2002). Effect of oceanic uptake on
- atmospheric lifetimes of selected trace gases. Journal of Geophysical
- 1085 Research: Atmospheres, 107(D20), ACH-1.
- Zhang, G., Yao, B., Vollmer, M. K., Montzka, S. A., Mühle, J., Weiss, R. F., et al.
- 1087 (2017). Ambient mixing ratios of atmospheric halogenated compounds at five
- background stations in China. Atmospheric Environment, 160, 55–69.
- 1089 Zhang, W., Jiao, Y., Zhu, R., Rhew, R. C., Sun, B., & Dai, H. (2021). Chloroform
- 1090 (CHCl₃) emissions from coastal Antarctic tundra. Geophysical Research
- 1091 Letters, 48(18), e2021GL093811.
- Zhang, Y. L., Guo, H., Wang, X. M., Simpson, I. J., Barletta, B., Blake, D. R., et al.
- 1093 (2010). Emission patterns and spatiotemporal variations of halocarbons in the
- Pearl River Delta region, southern China. Journal of Geophysical Research:
- 1095 Atmospheres, 115(D15).
- 1096 Zheng, P., Chen, T., Dong, C., Liu, Y., Li, H., Han, G., et al. (2019).
- 1097 Characteristics and sources of halogenated hydrocarbons in the Yellow River
- Delta region, northern China. Atmospheric Research, 225, 70-80.
- 1099 Zheng, J., Yu, Y., Mo, Z., Zhang, Z., Wang, X., Yin, S., et al. (2013). Industrial
- sector-based volatile organic compound (VOC) source profiles measured in
- manufacturing facilities in the Pearl River Delta, China. Science of the total
- environment, 456, 127-136.

FIGURE CAPTIONS

1103

1127

Fig. 1. (a) Locations of sampling stations (orange diamonds represent atmospheric 1104 sampling stations; SDZ: Shangdianzi background station; GSN: Gosan station). 1105 VCHCs for the GSN were obtained from AGAGE 1106 data network (https://agage.mit.edu/), and for the SDZ were derived from Yi et al. (2023). (b) A 1107 schematic map of the major currents of the Western Pacific. (c) Cluster analysis of 1108 96-h backward trajectories for different stations over the Western Pacific. The 1109 ensemble 96-h back-trajectories were within the lower troposphere above 100 m. 1110 1111 Fig. 2. Latitudinal distributions of SST, salinity, and Chl-a, and surface seawater and atmospheric concentrations of CCl₄, CHCl₃, CH₃CCl₃, and C₂HCl₃, along with 1112 1113 wind speed in the Western Pacific. 1114 Fig. 3. Distributions of CCl₄, CH₃CCl₃, CHCl₃, and C₂HCl₃ in the marine atmospheric boundary layer of the Western Pacific. 1115 Fig. 4. Saturation anomaly of CCl₄, CH₃CCl₃, CHCl₃, and C₂HCl₃ in the Western 1116 1117 Pacific. Fig. 5. Sea-air fluxes of CCl₄, CH₃CCl₃, CHCl₃, and C₂HCl₃, along with wind 1118 speeds in the Western Pacific. 1119 Fig. 6. Relationships between sea-air fluxes of VCHCs and wind speed, SST, and 1120 1121 VCHCs concentrations in seawater and the atmosphere. 1122 Fig. 7. (a) Interannual variations of wind speed, SST, and Chl-a concentration in the study area during 2019. (b) Interannual variability of CCl₄ at the GSN site in 1123 2019 compared with the global mean. (c) Interannual variability of CH₃CCl₃ at the 1124 1125 global scale in 2019. Wind speed data were obtained from the ERA5 reanalysis (Hersbach et al., 2020), SST data from the ECCO2 cube92 dataset (Menemenlis et 1126

al., 2008), and Chl-a data from the NASA Ocean Biology Processing Group

- 1128 (2022). Atmospheric CCl₄ and CH₃CCl₃ data were obtained from the AGAGE 1129 network (https://agage.mit.edu/). Shaded areas indicate the cruise sampling
- periods.
- 1131 **Fig. 8.** Schematic diagram of key processes and factors controlling the production,
- distribution, and sea-air interactions of VCHCs in the Western Pacific.

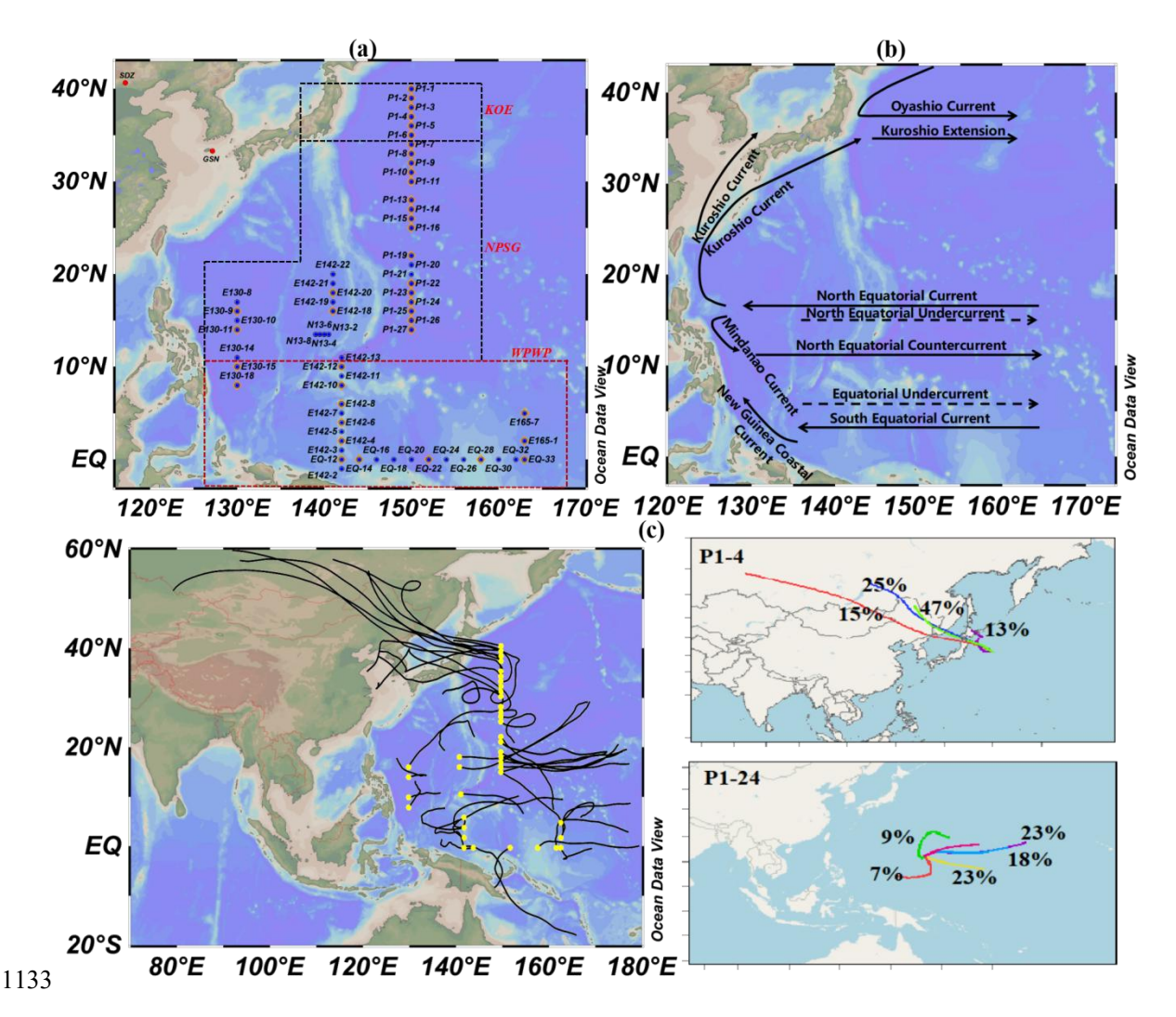


Fig. 1. (a) Locations of sampling stations (orange diamonds represent atmospheric sampling stations; SDZ: Shangdianzi background station; GSN: Gosan station). VCHCs data for the GSN were obtained from AGAGE network (https://agage.mit.edu/), and for the SDZ were derived from Yi et al. (2023). (b) A schematic map of the major currents of the Western Pacific. (c) Cluster analysis of 96-h backward trajectories for different stations over the Western Pacific. The ensemble 96-h back-trajectories were within the lower troposphere above 100 m.

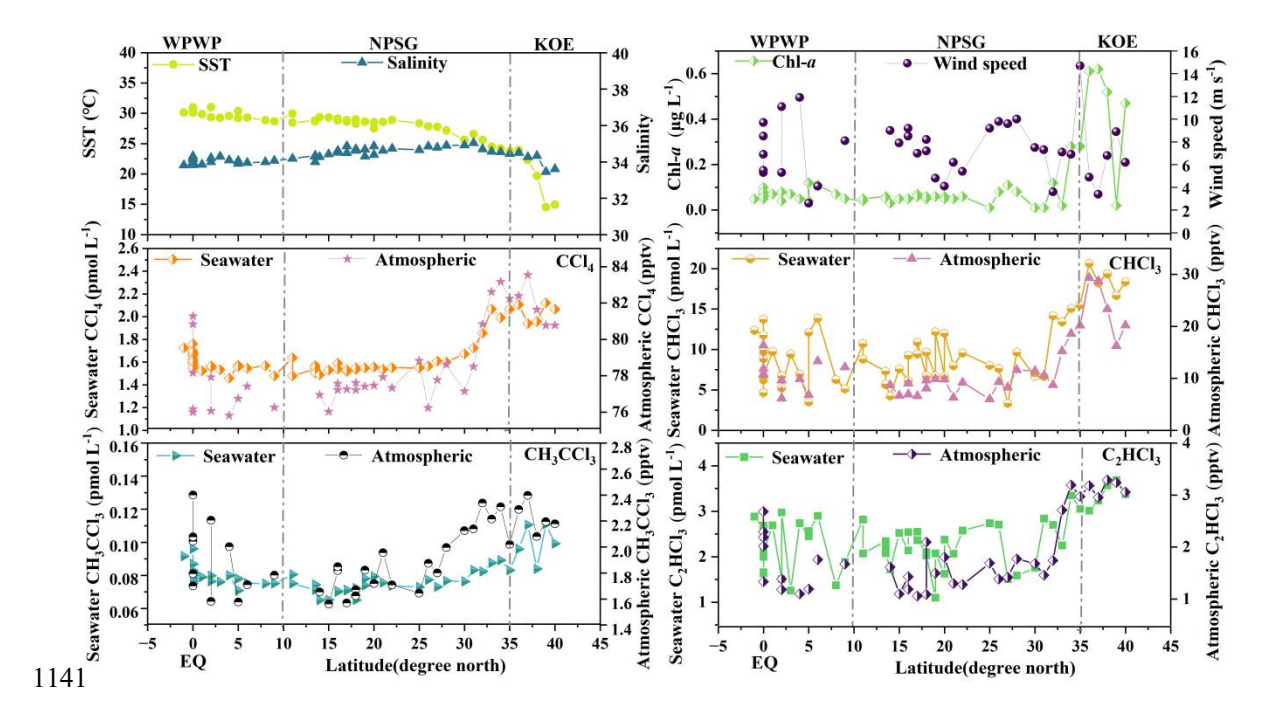


Fig. 2. Latitudinal distributions of SST, salinity, and Chl-*a*, and surface seawater and atmospheric concentrations of CCl₄, CHCl₃, CH₃CCl₃, and C₂HCl₃, along with wind speed in the Western Pacific.

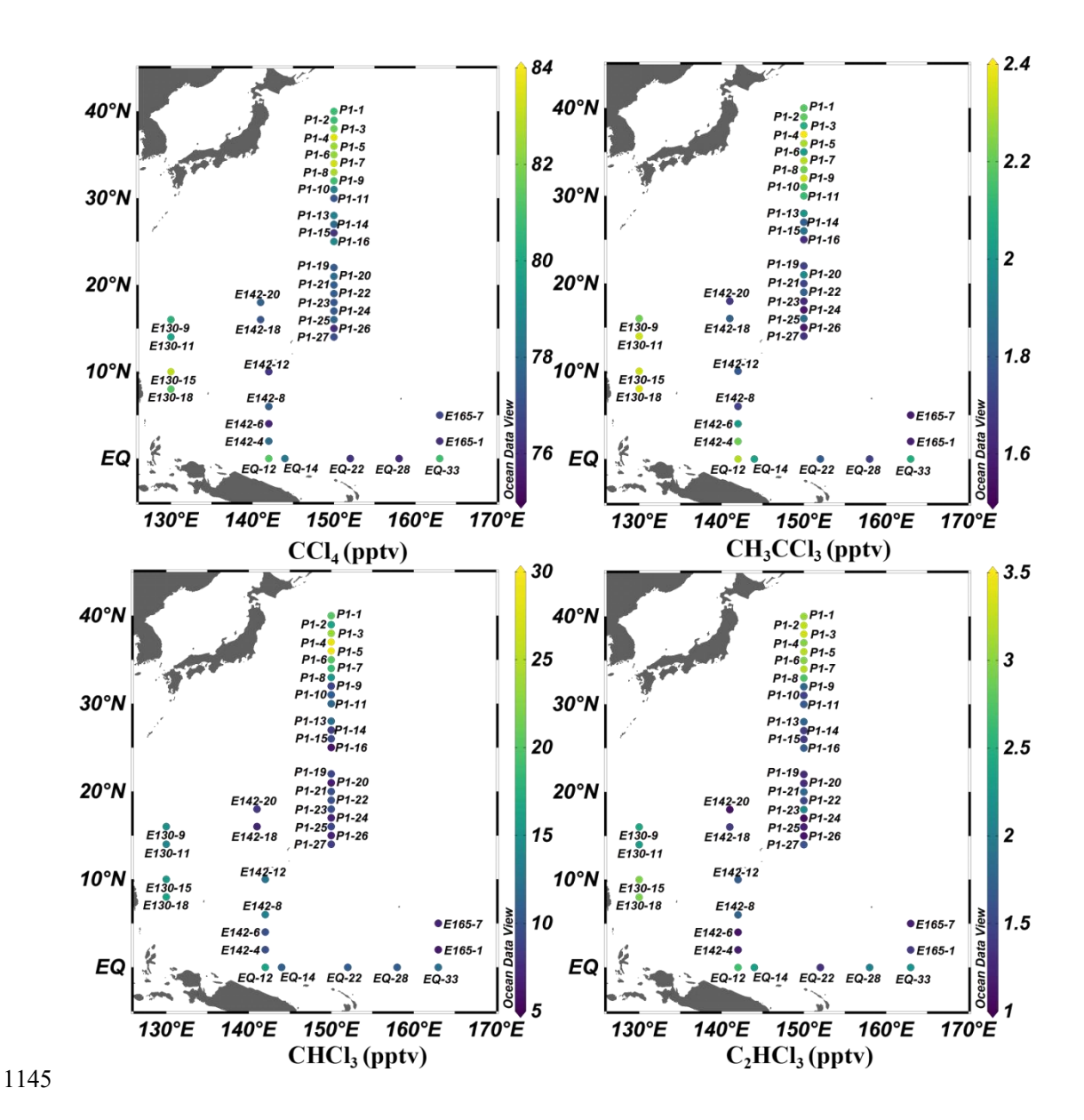


Fig. 3. Distributions of CCl₄, CH₃CCl₃, CHCl₃, and C₂HCl₃ in the marine atmospheric boundary layer of the Western Pacific.

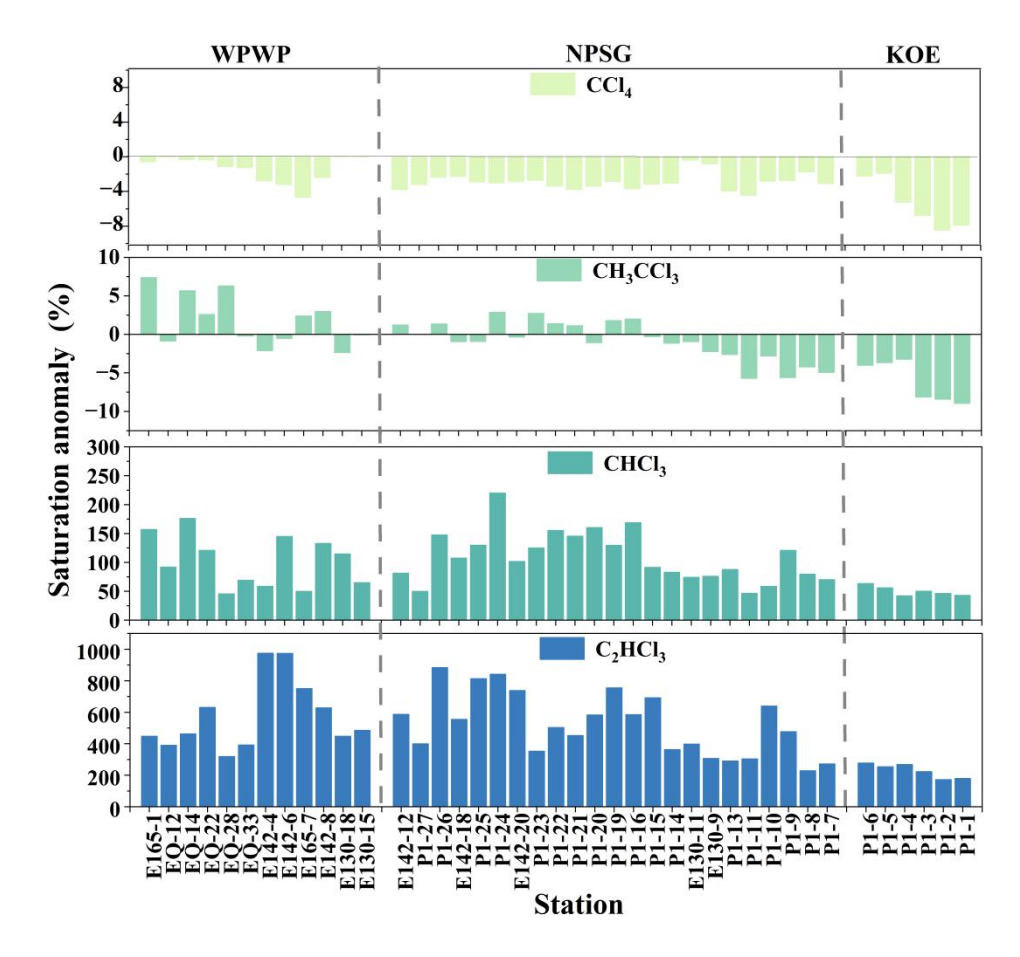


Fig. 4. Saturation anomaly of CCl₄, CH₃CCl₃, CHCl₃, and C₂HCl₃ in the Western Pacific.

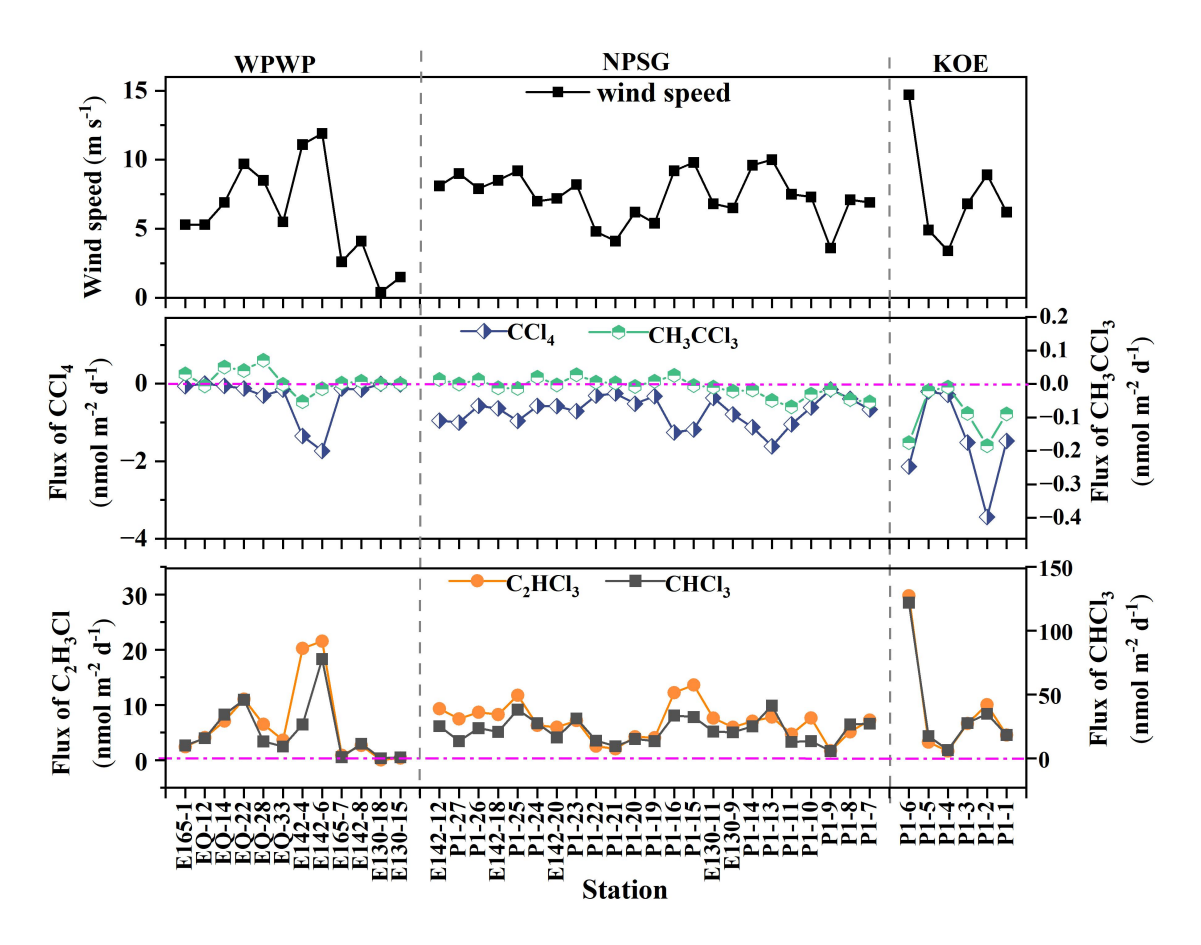


Fig. 5. Sea-air fluxes of CCl₄, CH₃CCl₃, CHCl₃, and C₂HCl₃, along with wind speeds in the Western Pacific.

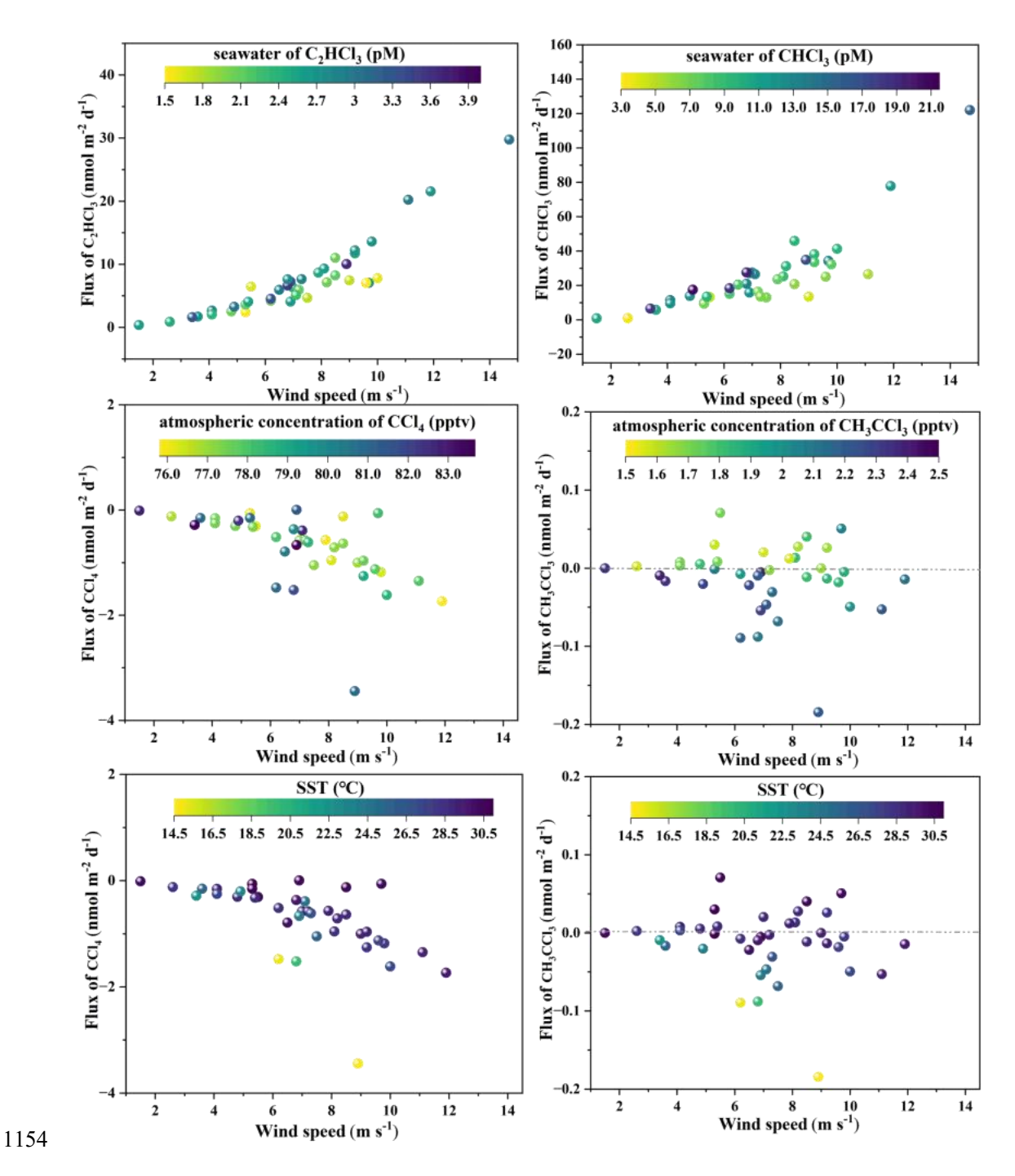


Fig. 6. Relationships between sea-air fluxes of VCHCs and wind speed, SST, and VCHCs concentrations in seawater and the atmosphere.

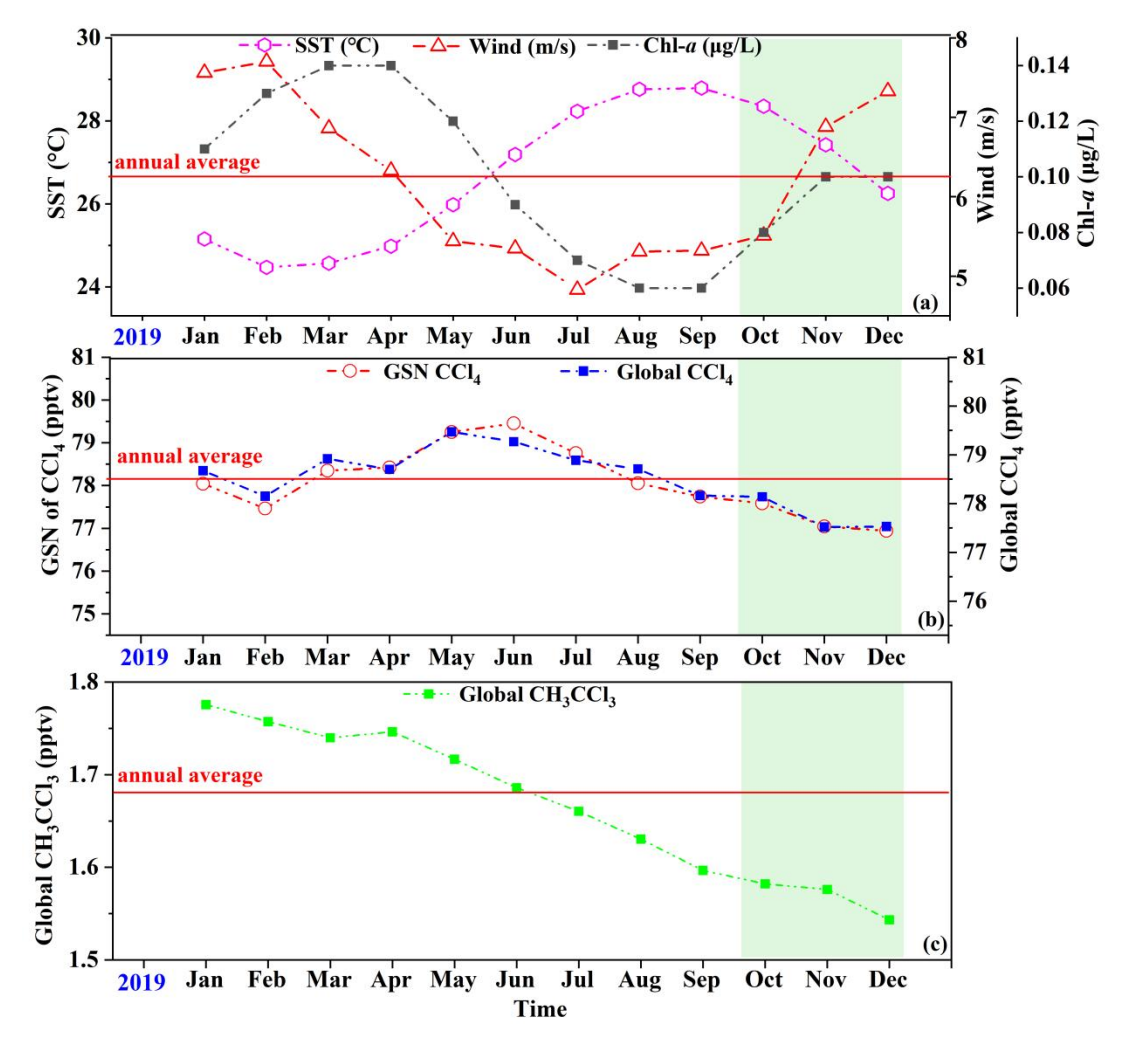


Fig. 7. (a) Interannual variations of wind speed, SST, and Chl-*a* concentration in the study area during 2019. (b) Interannual variability of CCl₄ at the GSN site in 2019 compared with the global mean. (c) Interannual variability of CH₃CCl₃ at the global scale in 2019. Wind speed data were obtained from the ERA5 reanalysis (Hersbach et al., 2020), SST data from the ECCO2 cube92 dataset (Menemenlis et al., 2008), and Chl-*a* data from the NASA Ocean Biology Processing Group (2022). Atmospheric CCl₄ and CH₃CCl₃ data were obtained from the AGAGE network (https://agage.mit.edu/). Shaded areas indicate the cruise sampling periods.

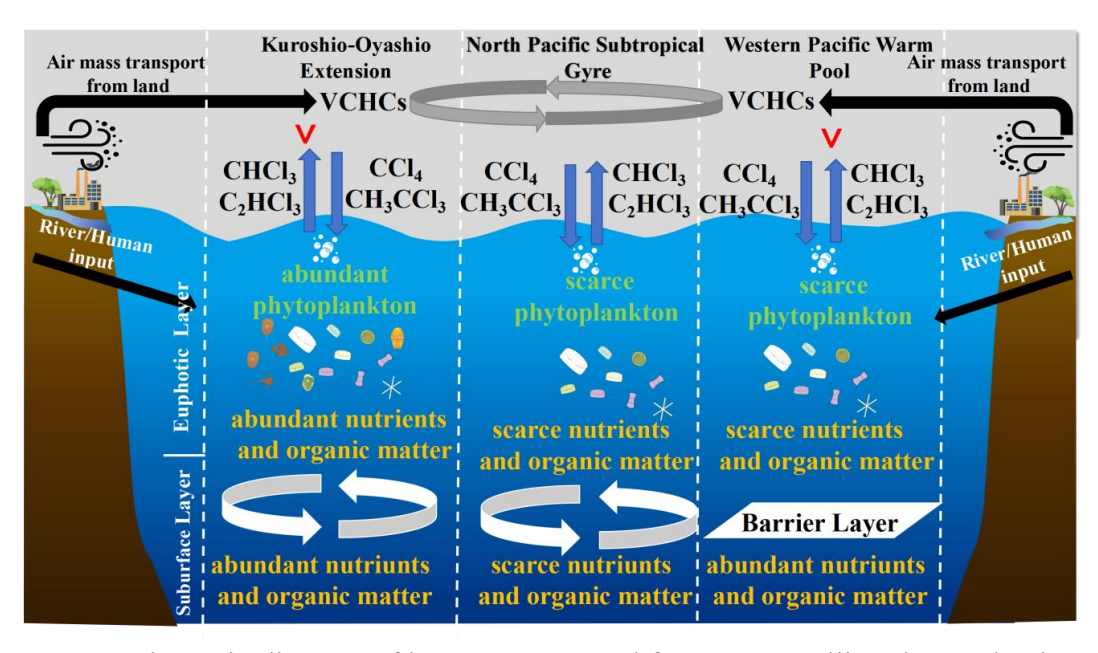


Fig. 8. Schematic diagram of key processes and factors controlling the production,

distribution, and sea-air interactions of VCHCs in the Western Pacific.

1167